Cell

EBV infection and HLA-DR15 jointly drive multiple sclerosis by myelin peptide presentation

Graphical abstract

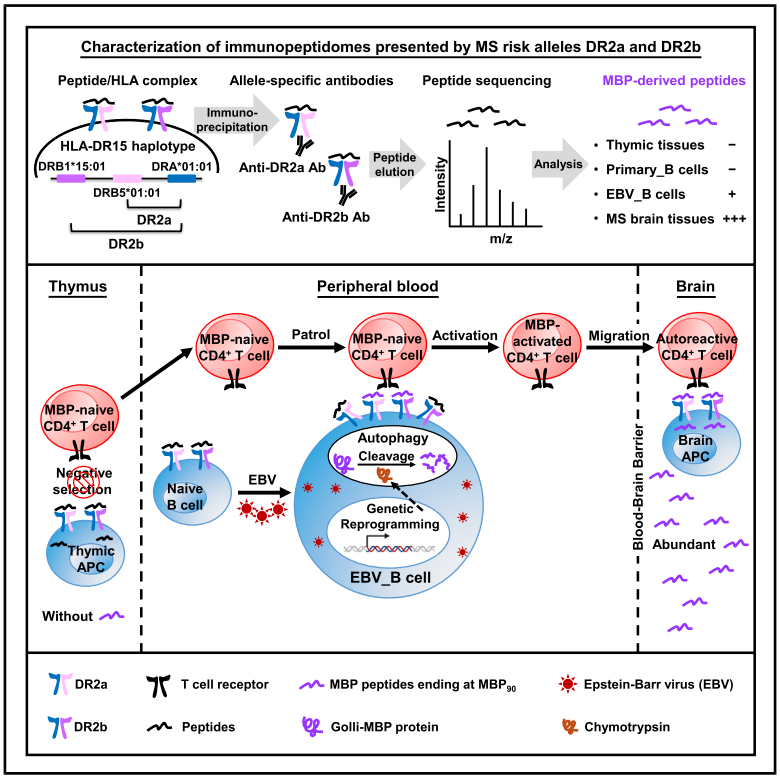

Highlights

- EBV infection alters the transcriptome and immunopeptidome of B cells
- EBV-infected B cells present MBP peptides on surface HLA-DR15 molecules
- MBP peptides on EBV-infected B cells are also presented on HLA-DR15 in MS brain tissue
- MBP peptide-reactive memory CD4$^+$ T cells exist in the periphery and CSF of MS patients

Authors

Jian Wang, Yuhan Qiu, Zoe Marti, ..., Richard Reynolds, Juliane Walz, Roland Martin

Correspondence

ustcwj@ustc.edu.cn (J.W.), roland.martin@uzh.ch (R.M.)

In brief

EBV infection alters the transcriptome of B cells, which leads to presentation of MBP peptides on HLA-DR15 molecules. MBP peptide-specific CD4$^+$ T cells are found in the peripheral immune compartment and CNS, where they recognize the same MBP peptides on HLA-DR15 molecules.

Wang et al., 2026, Cell *189*, 569–584
January 22, 2026
https://doi.org/10.1016/j.cell.2025.12.046

CellPress

Cell

CellPress
OPEN ACCESS

Article

EBV infection and HLA-DR15 jointly drive multiple sclerosis by myelin peptide presentation

Jian Wang,[1,*] Yuhan Qiu,[2,21] Zoe Marti,[2,3,21] Fengqi Li,[1,4,21] Marcel Wacker,[5,6] Pietro Oldrati,[3] Lena Mühlenbruch,[5,6,7] Linlin Jin,[1] Hongxia Zhang,[1,4] Wen Xu,[1] Tingting Li,[1,8] Bernd Roschitzki,[9] Wolfgang Faigle,[10,11] Yingjun Liu,[12] Julie T. Nguyen,[13] Jar-How Lee,[13] Veronika Haunerdinger,[14] Mathias Hauri-Hohl,[14] Frank Momburg,[15] Jens Bauer,[5,6,7] Hans-Georg Rammensee,[6,7,16] Mireia Sospedra,[3,10] Roberta Magliozzi,[17,18] Richard Reynolds,[17] Juliane Walz,[5,6,7,19] and Roland Martin[2,3,10,20,22,*]

[1]State Key Laboratory of Immune Response and Immunotherapy, Department of Neurology, The First Affiliated Hospital of USTC, Center for Advanced Interdisciplinary Science and Biomedicine of IHM, Division of Life Sciences and Medicine, University of Science and Technology of China, 230001 Hefei, China
[2]Institute of Experimental Immunology, University of Zurich, 8057 Zurich, Switzerland
[3]Cellerys AG, Wagistrasse 21, 8952 Schlieren, Switzerland
[4]Institute of Health and Medicine, Hefei Comprehensive National Science Center, 230061 Hefei, China
[5]Department of Peptide-Based Immunotherapy, Institute of Immunology, University and University Hospital Tübingen, 72076 Tübingen, Germany
[6]Cluster of Excellence iFIT (EXC 2180) "Image-Guided and Functionally Instructed Tumor Therapies", University of Tübingen, 72076 Tübingen, Germany
[7]German Cancer Consortium (DKTK) and German Cancer Research Center (DKFZ), Partner Site Tübingen, 72076 Tübingen, Germany
[8]Department of Clinical Laboratory, First Affiliated Hospital of Anhui Medical University, 230022 Hefei, China
[9]Functional Genomics Center Zurich, Swiss Federal Institute of Technology (ETHZ) and University of Zurich (UZH), Winterthurerstrasse 190, 8057 Zurich, Switzerland
[10]Neuroimmunology and MS Research, Neurology Clinic, University Hospital Zurich, University of Zurich, 8091 Zurich, Switzerland
[11]Institut Curie, PSL University, Inserm U932, Immunity and Cancer, 75005 Paris, France
[12]Faculty of Life and Health Sciences, Shenzhen University of Advanced Technology (SUAT), 518107 Shenzhen, China
[13]One Lambda, Inc., a part of Transplant Diagnostics Thermo Fisher Scientific, 22801 Roscoe Blvd., West Hills, CA 91304, USA
[14]Pediatric Stem Cell Transplantation, University Children's Hospital Zurich, 8032 Zurich, Switzerland
[15]Department of Medical Oncology, National Center for Tumor Diseases (NCT) Heidelberg, Heidelberg University Hospital, 69120 Heidelberg, Germany
[16]Institute of Immunology, University of Tübingen, 72076 Tübingen, Germany
[17]Division of Neuroscience, Department of Brain Sciences, Imperial College London, London, UK
[18]Department of Neurosciences, Biomedicine and Movement Sciences, University of Verona, 37124 Verona, Italy
[19]Clinical Collaboration Unit Translational Immunology, Department of Internal Medicine, University Hospital Tübingen, 72076 Tübingen, Germany
[20]Therapeutic Immune Design Unit, Department of Clinical Neuroscience, Karolinska Institute, Center for Molecular Medicine, 17177 Stockholm, Sweden
[21]These authors contributed equally
[22]Lead contact
*Correspondence: ustcwj@ustc.edu.cn (J.W.), roland.martin@uzh.ch (R.M.)
https://doi.org/10.1016/j.cell.2025.12.046

SUMMARY

Epstein-Barr virus (EBV) is involved in causing and probably also in perpetuating multiple sclerosis (MS). Among several mechanisms of how EBV may contribute are transcriptome alterations, including changes of antigen processing and preferential presentation of both viral and self-antigens. Here, we report that EBV reprograms the transcriptome and immunopeptidome presented on the MS-associated human leukocyte antigen (HLA)-DR15 molecules of infected B cells. Identical myelin basic protein (MBP) peptides were found to be presented on both EBV-infected B cells and MS brain tissue but not primary B cells and thymic tissue. Peripheral memory and cerebrospinal fluid (CSF)-derived $CD4^+$ T cells of HLA-$DR15^+$ MS patients responded to MBP peptides, $MBP_{(78–90)}$ and/or $MBP_{(83–90)}$, and T cell clones raised with these peptides recognized all MBP peptides ending at amino acid MBP_{90} in MS brain tissue. Our study provides a new mechanistic link for how the environmental and genetic risk factors, EBV infection and HLA-DR15 haplotype, may contribute jointly to MS.

INTRODUCTION

Multiple sclerosis (MS) is a chronic autoimmune disease of the central nervous system (CNS) and is characterized by autoimmune inflammation, axonal and neuronal damage, de- and remyelination, glial activation, and metabolic alterations.[1,2] The causes of MS involve both environmental influences and genetic factors.[3,4]

Numerous studies implicate Epstein-Barr virus (EBV) infection as a trigger of MS.[5–8] EBV is a ubiquitous human herpesvirus with B cell tropism leading to lifelong latent infection of memory B cells. 90%–95% of healthy adults are infected with EBV, and MS patients are close to 100% EBV positive or turn positive at disease onset.[5] EBV infection may contribute to MS development and/or sustaining it by several mechanisms,[6,9] including antibody- and T cell cross-recognition between EBV proteins and myelin- or non-myelin MS autoantigens, i.e., molecular mimicry,[10–17] by changing the transcriptional profile of B cells,[18–20] and by inducing B cell trafficking to the CNS and other tissues.[21–24] Regarding autoreactive T cell responses in MS, it is not well understood how EBV-induced changes in B cells may contribute, but molecular mimicry between EBV and self-peptides is currently favored.

Almost all people are infected with EBV, but only approximately 1/1,000 develop MS. Therefore, factors other than EBV infection must contribute to MS development, particularly genetic susceptibility.[4] Among these, the human leukocyte antigen (HLA)-DR15 haplotype is most important and may contribute up to 60% of the total genetic risk for MS.[25] The HLA-DR15 molecules DRA*01:01/DRB5*01:01 (DR2a) and DRA*01:01/DRB1*15:01 (DR2b) present peptides to T cell receptors (TCRs) to activate $CD4^+$ T cells, which is consistent with the fact that MS is a $CD4^+$ T cell-mediated autoimmune disease.[1,26,27] Several pieces of evidence, including increased anti-EBV nuclear antigen 1 (EBNA1) antibodies, indicate that EBV infection, particularly infectious mononucleosis, and the HLA-DR15 haplotype synergistically increase MS risk.[3,28–30]

As described above, EBV establishes a latent infection in B cells, driving their activation and differentiation while altering their transcriptome, including the expression of multiple MS risk genes and of autoantigens.[20,31,32] Here, we examined how EBV-associated transcriptional alterations change the immunopeptidomes, that is, the peptides presented by the two HLA-DR15 allomorphs, DR2a and DR2b, in EBV-infected B cells and MS brain tissue, and whether these might be related to MS.

Acquiring EBV-infected B cells from MS patients would be an important step. However, EBV-infected B cells are very rare during latent infection, i.e., approximately 2–10 per million circulating B cells or lower, both in healthy carriers and MS patients.[33] Thus, one cannot isolate and analyze them directly, at least not in sufficient numbers for immunopeptidomics, which requires 20 million or more cells. We therefore utilized a widely used model of latent EBV infection, i.e., infecting primary B cells with EBV to generate EBV-transformed B cells *in vitro*,[34] which may mimic an asymptomatic primary infection.[19] Previous studies found that the response to the latency III program of EBV infection contributes to MS susceptibility.[35] The latency III program is characterized by expression of all EBV latency genes, such as EBNA1/2/3 and latent membrane protein 1/2 (LMP1/2), and EBV-transformed B cells show this pattern *in vitro*.[36] Hence, we utilized the EBV-transformed B cell lines in this study as a surrogate for the latent state of EBV infection.

RESULTS

EBV infection changes the immunopeptidome presented by HLA-DR15 molecules of B cells

To examine how EBV infection changes the B cell immunopeptidomes, EBV-transformed B cell lines (hereafter referred to as EBV_B cells) were generated[37] from 3 HLA-DR15$^+$ relapsing-remitting MS (RRMS) patients (Table S1). Consistent with previous reports,[18,32] the transcriptome of the EBV_B cells differed significantly from that of primary B cells (hereafter referred to as primary_B cells) (Figures 1A, S1A, and S1B), and proteasome-related genes showed the greatest increase (Figure S1C). The top upregulated genes in EBV_B cells play a role in biological processes of DNA replication/repair, metabolic, and amino acid metabolism processes, and the downregulated ones in autoimmune, allergic, and parasitic diseases as well as B cell receptor signaling and graft-versus-host disease (Figure S1C). Further, EBV_B cells significantly increased the surface expression of both DR2a and DR2b molecules compared with primary_B cells (Figure 1B). We then used the DR2a- and DR2b-specific monoclonal antibodies to specifically immunoprecipitate the two HLA-DR15 molecules of EBV_B cells, elute bound peptides, and analyze them by mass spectrometry-based sequencing. The total numbers of peptides eluted from DR2a and DR2b were sufficiently broad and comparable between primary_B cells[10] and EBV_B cells (Figure 1C; Table S2). Unique peptides from DR2a and DR2b of EBV_B cells were increased compared with primary_B cells, albeit not significantly (Figure 1D). The amino acid preferences at deduced anchor positions p1, 4, and 9 for DR2a or p1, 4, and 7 for DR2b were similar between primary_B cells[10] and EBV_B cells (Figure 1E), but DR2a- or DR2b-presented unique peptides and source proteins showed limited overlap (Figure 1F), indicating that, consistent with the transcriptomic changes, EBV infection also alters the HLA-DR15-presented immunopeptidomes.

MBP-derived peptides are eluted from HLA-DR15 molecules of EBV-infected B cells

Next, we analyzed the EBV_B cell-specific peptides presented by HLA-DR15 molecules. Unexpectedly, four peptides from one of the major myelin proteins and MS autoantigens, myelin basic protein (MBP), i.e., $MBP_{(78–90)}$, $MBP_{(83–90)}$, $MBP_{(91–106)}$, and $MBP_{(91–114)}$, were eluted from DR2a and/or DR2b of all three EBV_B cell samples, but not from primary_B cells (Figure 1G). Although additional MS autoantigens, including crystallin alpha B (CRYAB),[15,38] RAS guanyl releasing protein 2 (RASGRP2),[39] and reticulon 3 (RTN3),[40] were also detected at the mRNA level in EBV_B cells and/or primary_B cells (Figure 1H), we did not find peptides from these proteins in the immunopeptidomes of DR2a or DR2b of either cells[10] (Table S2). To examine if presentation of MBP peptides by HLA-DR15 molecules in EBV_B cells was associated with disease status, we generated EBV_B cells from 4 HLA-DR15$^+$ healthy donors (HDs) (Table S1) and performed transcriptome,

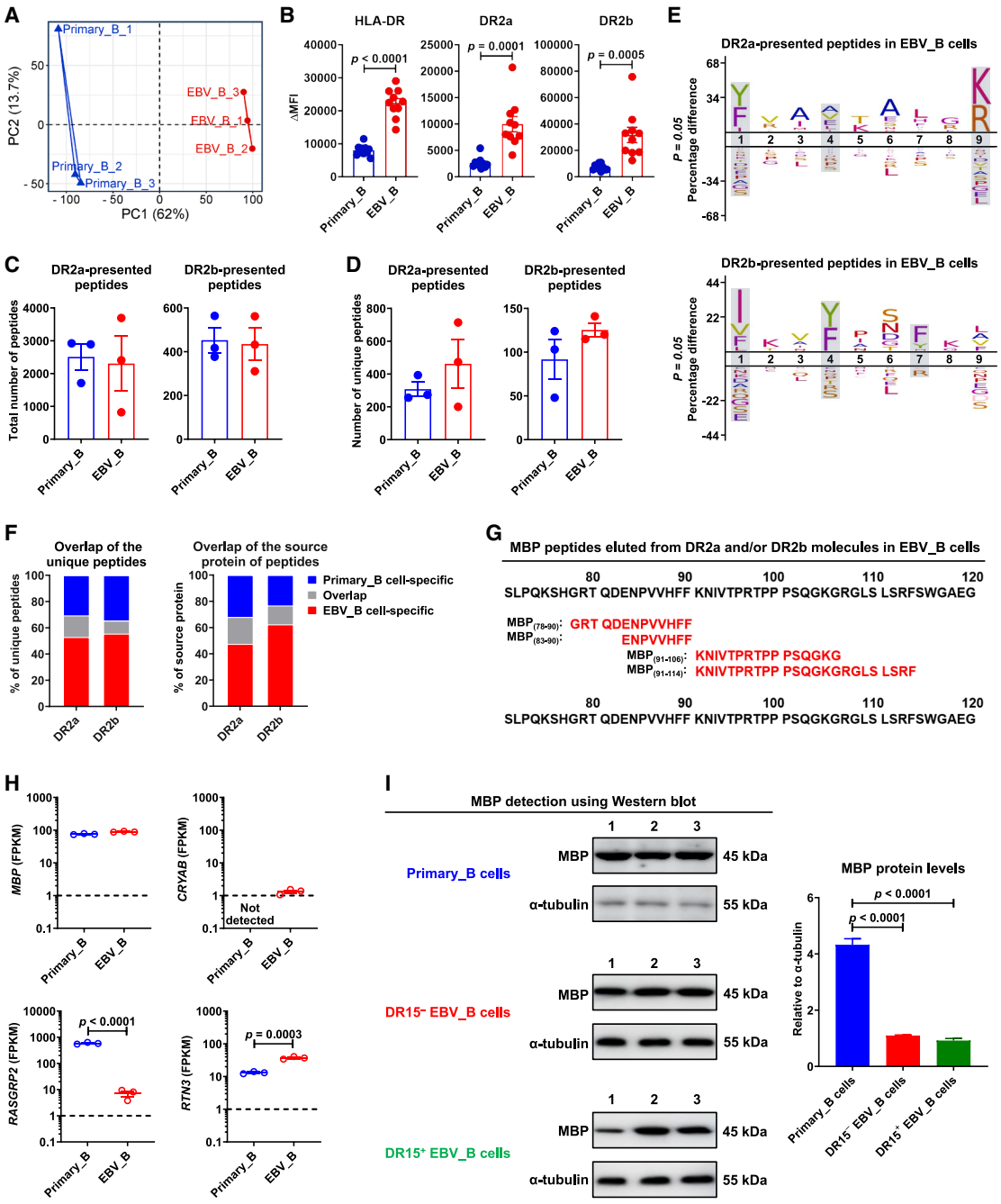

Figure 1. MBP peptides are identified in DR2a/DR2b-presented peptides in EBV_B cells

(A) Principal-component analysis (PCA) of transcripts collected from 3 primary_B cells and their corresponding EBV_B cells.

(B) Comparison of the expression levels of HLA-DR, DR2a, and DR2b on primary_B cells and EBV_B cells. ΔMFI (mean fluorescence intensity) = MFI (marker) − MFI (isotype).

(C) Comparison of the total number of peptides eluted from DR2a and DR2b between primary_B cells and EBV_B cells.

(D) Comparison of the number of unique peptides presented by DR2a and DR2b between primary_B cells and EBV_B cells.

(E) Nine amino acid binding motifs of DR2a- and DR2b-presented peptides in EBV_B cells based on NetMHCII 2.3 analysis and visualization by iceLogo. Putative peptide anchor positions for DR2a and DR2b are highlighted in gray.

(F) Overlap of DR2a- and DR2b-presented unique peptides and their source proteins between primary_B cells and EBV_B cells.

(G) Four MBP peptides eluted from DR2a and DR2b in EBV_B cells.

(legend continued on next page)

proteome, and immunopeptidome analyses. We did not find significant differences in the transcriptomes and proteomes between EBV_B cells from HDs and MS patients (Figures S2A and S2B), but the comparison of DR2a- or DR2b-presented unique peptides and source proteins showed limited overlap (Figure S2C; Tables S2 and S3), which might be attributed to interindividual heterogeneity of DR2a- and DR2b-presented peptides among EBV_B cells from different HDs or MS patients (Figure S2D). Further, we identified only one of the four above MBP peptides, i.e., $MBP_{(78–90)}$, in the DR2a-presented immunopeptidome of one of the four HD EBV_B cell samples (Figure S2E). Based on these data, we currently assume that the EBV-induced changes of the transcriptome and proteome of EBV_B cells are largely similar, but we cannot exclude differences in the immunopeptidomes of EBV_B cells in HDs versus MS patients.

To identify the source of the MBP peptides, which we assumed to be Golli-MBP in B cells, we applied both polymerase chain reaction (PCR) and proteomics and indeed found both Golli-MBP transcripts (Figure S3A) as well as peptides that are only present in the Golli region of the longest MBP isoform, i.e., in the N-terminal portion prior to the start of the brain isoform (Figure S3B). We also detected MBP protein in both primary_B cells and EBV_B cells by western blot and at significantly lower levels in EBV_B cells (Figure 1I), indicating degradation of MBP in EBV_B cells by altered processing. Enzymes related to antigen processing, including some cathepsins, almost all endosomal proteases, including a larger number of the immunoproteasome members, and ERAP1/2, were upregulated in EBV_B cells (Figure S1D), and these changes appear to begin in B cells on the first day after EBV infection.[18] Of those, proteasome 20S subunit beta 8 (PSMB8) and its chymotrypsin-like cleavage are the most likely candidates to cleave MBP after the two phenylalanine (F) residues at positions 89 and 90.[41] Indeed, high PSMB8 expression was detected at both transcriptional and protein levels in both primary_B cells and EBV_B cells (Figures S1D and S3C). Among different processing paths, including proteasome-mediated digestion, chaperone-mediated autophagy, and autophagy, the latter was shown to be important for processing and presentation of self- and viral antigens by major histocompatibility complex class II (MHC class II) molecules.[42,43] Consistently, autophagy was significantly increased in EBV_B cells (Figure S3D), which may act in concert with PSMB8 to degrade MBP in autophagic lysosomes and subsequent presentation of MBP peptides by HLA-DR15 molecules. Therefore, these EBV-induced alterations of antigen processing and presentation may explain the observation of intracellular protein-derived peptides, including MBP, on both DR2a and DR2b.

HLA-DR15-presented MBP peptides in EBV_B cells are also presented in MS brain tissue

To explore whether the same MBP peptides presented by EBV_B cells are also presented in MS brain, we analyzed the DR2a- and DR2b-presented immunopeptidome in brain tissues with both inflammatory meningeal and parenchymal lesions of 4 HLA-$DR15^+$ MS patients (Figure 2A; Table S4). Immunopeptidome analyses showed similar amino acid anchor preferences for DR2a or DR2b as peptides eluted from EBV_B cells, but brain-derived peptides were enriched for basic amino acids in non-MHC anchor positions (Figures 1E and 2B). DR2a- or DR2b-presented unique peptides and source proteins showed limited overlap between EBV_B cells and MS brain tissues (Figure 2C). Further, we found several peptides derived from proteins that are specifically or highly expressed in brain tissues, such as MBP, glial fibrillary acidic protein (GFAP), and fibroblast growth factor 3 (FGF3) (Figure 2D), and many DR2a- and DR2b-presented peptides derived from MBP and GFAP (Figure 2E). MBP-derived peptides accounted for 5.94% of the DR2a- and 5.32% of the DR2b-presented immunopeptidomes, respectively (Figure 2F), and covered nearly the entire sequence of the most abundant MBP brain isoform (Figure S4). Interestingly, three of the four EBV_B cell-eluted MBP peptides (Figure 1G), i.e., $MBP_{(83–90)}$, $MBP_{(91–106)}$, and $MBP_{(91–114)}$, were also detected in DR2a- and DR2b-presented immunopeptidomes from MS brain tissues (Figure 2G). We currently do not know where the MBP peptides that are presented on DR2a and DR2b molecules in the brain come from, but we assume that they are processed by resident microglia or macrophages that have taken up myelin debris. This notion is supported by the observation that we found only peptides from the brain isoform (Figure S4; Table S4). Considering that MBP is a well-known MS autoantigen, we focused subsequent experiments on characterizing MBP peptides.

Memory $CD4^+$ T cells in HLA-$DR15^+$ MS patients respond to MBP peptides

Based on the above findings and previous reports that B cells function as antigen-presenting cells (APCs) in MS,[10,39,44,45] we hypothesized that EBV infection enables HLA-DR15 to present MBP-derived peptides on B cells, subsequently activates peripheral autoreactive $CD4^+$ T cells, which may then recognize MBP peptides in the brain and contribute to disease. Therefore, we first tested the response of peripheral blood mononuclear cells (PBMCs) from HLA-$DR15^+$ HDs and MS patients against MBP peptides. To reduce background autoproliferation,[10,39] we used CD45RA-depleted ($CD45RA^-$) PBMCs, which include monocytes and memory T cells but not B and naive T cells. We tested 16 HDs (HD-1∼16) and 16 RRMS patients (RRMS-1∼16) (Table S5) with individual or pooled MBP peptides. 10 of 14 HDs and 14 of 15 RRMS patient samples showed robust reactivity to EBV EBNA1 protein or peptides, indicating prior EBV infection (Table S5), which is consistent with past reports.[5] $CD45RA^-$ PBMCs from RRMS patients responded robustly to individual peptides $MBP_{(78–90)}$ and $MBP_{(83–90)}$ as well as the peptide pool, whereas $CD45RA^-$ PBMCs from HDs rarely responded (Figure 3A). Among the 16

(H) The mRNA expression levels of known MS autoantigens MBP, CRYAB, RASGRP2, and RTN3 in primary_B cells and EBV_B cells. FPKM, fragments per kilobase million.

(I) Expression of MBP protein in primary_B cells, $DR15^-$ EBV_B cells, and $DR15^+$ EBV_B cells. Data are expressed as mean or mean ± SEM, and p values were determined by unpaired t test.

See also Figures S1–S3 and Tables S1, S2, and S3.

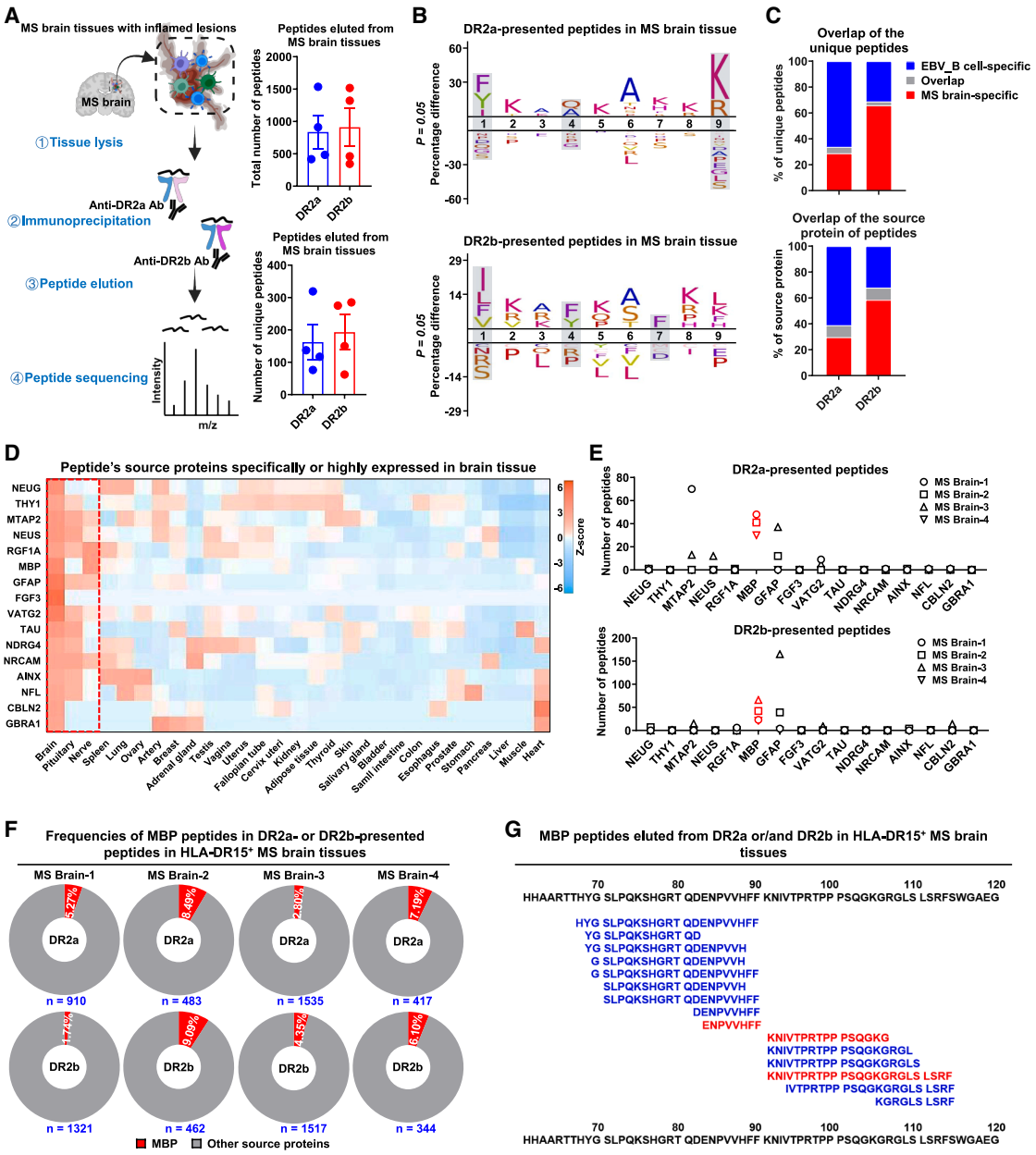

Figure 2. MBP peptides presented by EBV_B cells can also be found in DR2a/DR2b-presented peptides in MS brain tissues

(A) Workflow diagram for the identification of DR2a- and DR2b-presented peptides derived from human proteins in HLA-DR15^{+} RRMS brain tissues containing highly inflamed lesions. The total number of peptides and the number of unique peptides presented by DR2a and DR2b in MS brain tissues is shown.

(B) Nine amino acid binding motifs of DR2a- and DR2b-presented peptides in MS brain tissues.

(C) Overlap of DR2a- and DR2b-presented unique peptides and their source proteins between EBV_B cells and MS brain tissues.

(D) Enrichment of human tissue-specific genes among the source proteins of the peptides based on RNA-seq data across 29 human tissues from the Genotype-Tissue Expression (GTEx) dataset. Source proteins of DR2a- and DR2b-presented peptides specifically or highly expressed in brain tissues are shown.

(E) The number of DR2a- or DR2b-presented peptides from the indicated source proteins in 4 MS brain tissues.

(F) Proportions of MBP peptides in DR2a- or DR2b-presented peptides in MS brain tissues with respect to the total number of peptides eluted from each sample.

(G) MBP peptides eluted from DR2a and DR2b in MS brain tissues include three of four of the MBP peptides eluted from EBV_B cells. These shared three MBP peptides are highlighted in red.

Data are expressed as mean or mean ± SEM.

See also Figure S4 and Table S4.

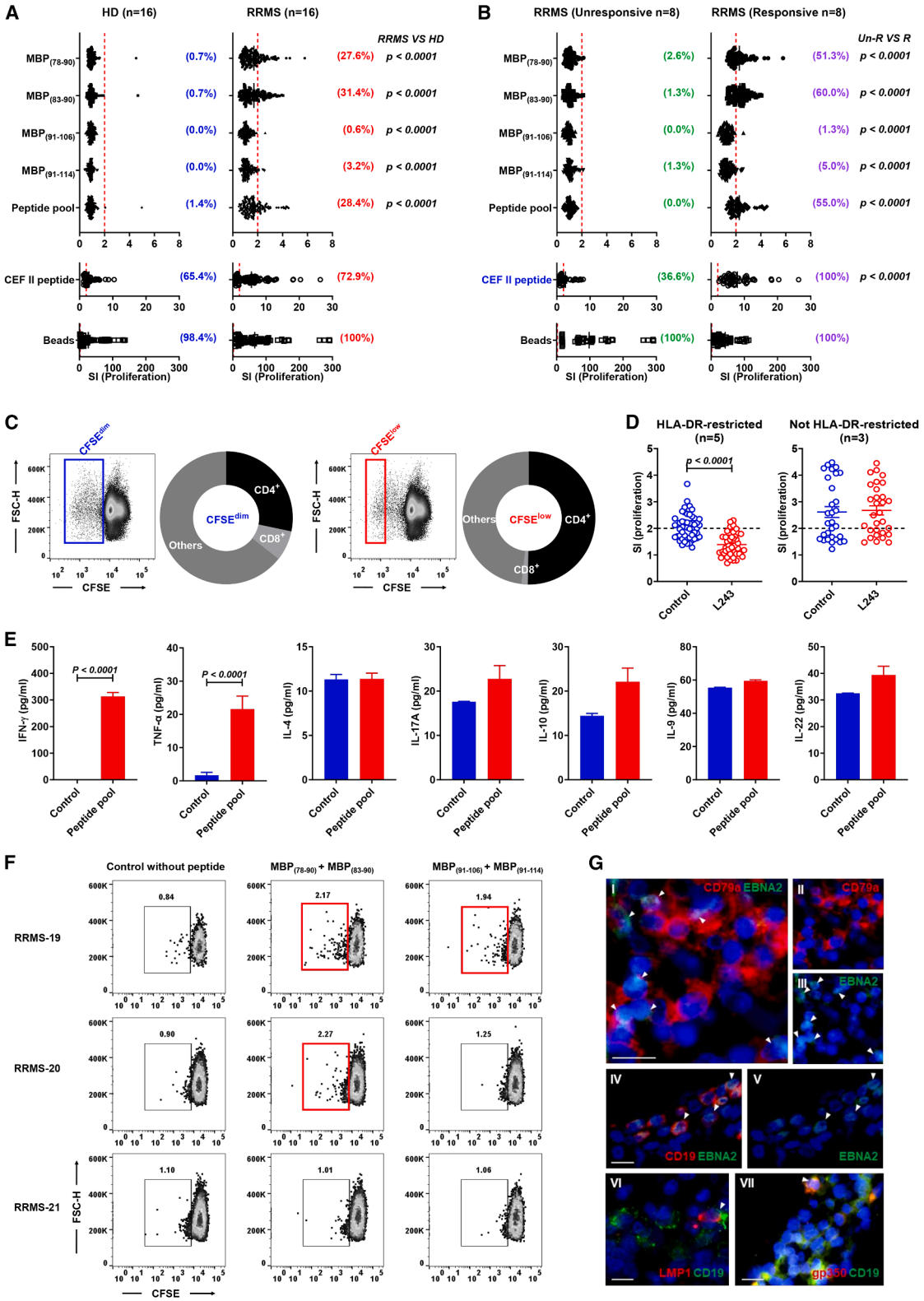

Figure 3. Increased reactivity of memory CD4⁺ T cells against MBP peptides eluted from EBV_B cells in MS patients

(A) CD45RA⁻ PBMCs from HLA-DR15⁺ HDs ($n = 16$) and RRMS patients ($n = 16$) were stimulated with the four MBP peptides individually or pooled. Proliferation of CD45RA⁻ PBMCs was measured after 7 days by ^{3}H-thymidine or BrdU incorporation assay. Proliferation relative to background is depicted as stimulatory index

(legend continued on next page)

RRMS samples, 8 responded to the MBP peptides, while 8 did not (Figure 3B). Unresponsive RRMS samples also responded less to the viral/bacterial CEF II peptide pool that includes 23 peptides from influenza A/B, tetanus, EBV, and cytomegalovirus (CMV) (Figure 3B). Among proliferating cells ($CFSE^{dim}$), memory $CD4^+$ T cells divided most ($CFSE^{low}$) (Figure 3C). To address presentation by HLA-DR molecules, we used the blocking pan-anti-HLA-DR antibody L243. In 5/8 MBP peptide-responsive RRMS samples, proliferation to MBP peptide pool stimulation could be blocked (Figure 3D), indicating involvement of TCR and MBP peptide/HLA-DR complex interactions. The lack of blocking in three samples (Figure 3D) may indicate that other HLA class II molecules than HLA-DR might also present MBP peptides. MBP peptide-responsive cells secreted high levels of the T helper 1 (Th1) cytokine interferon γ (IFN-γ), but not cytokines of other Th cell subsets (Figure 3E). Hence, proinflammatory MBP peptide-specific $CD4^+$ T cells exist in the peripheral blood of MS patients and are directed against $MBP_{(78–90)}$ and $MBP_{(83–90)}$.

Next, we were interested if MBP peptide-responsive T cells can also be found in the CNS compartment and tested the proliferation of cerebrospinal fluid (CSF)-derived $CD4^+$ T cells from three $HLA\text{-}DR15^+$ MS patients (Table S5), which had been expanded as bulk populations.[46] CFSE dilution assays revealed that CSF $CD4^+$ T cells from two of three individuals reacted against $MBP_{(78–90)}$ and $MBP_{(83–90)}$, and one individual against $MBP_{(91–106)}$ and $MBP_{(91–114)}$ (Figure 3F). Thus, autoreactive $CD4^+$ T cells recognizing MBP peptides are present in both peripheral blood and CSF of patients with MS. While still preliminary, immunohistochemical studies of MS brain tissue samples showed positive staining for the EBV latent proteins EBNA2, LMP1, and/or the structural protein gp350 in all four brain tissues we used for immunopeptidome analysis (Figure 2A), which indicates EBV infection and migration of virus-infected B cells into the CNS compartment (Figure 3G), consistent with a recent study.[24] Hence, we assume that the latter may be involved in stimulating EBV-specific and/or MBP peptide-specific T cells in the brain.

$MBP_{(78–90)}$ and $MBP_{(83–90)}$ are not eluted from HLA-DR15 molecules in thymus

Clonal deletion of high-avidity autoreactive T cells by negative selection in the thymus is the key mechanism of central tolerance, and negative selection relies on the expression of self-antigens in thymus.[47] Several previous studies have confirmed MBP expression in the human thymus.[48,49] We therefore examined MBP expression in thymic APCs. Indeed, MBP is expressed in thymic epithelial cells (TECs) but more highly in bone marrow-derived APCs, including thymic B cells, thymic dendritic cells (DCs), and thymic macrophages (Mø) (Figure 4A). A few other genes that are specifically or only found in brain tissues (Figure 2D) are also expressed to varying degrees in thymus (Figure 4A). To explore if $MBP_{(78–90)}$ and $MBP_{(83–90)}$ were presented by DR2a and DR2b in the thymus, we analyzed the immunopeptidome presented by DR2a and DR2b in thymic tissues of 4 $HLA\text{-}DR15^+$ HDs (Figure 4B). Peptides were eluted more from DR2a (3,500 on average) and less from DR2b (1,150 on average) (Figure 4B; Table S6). Of the DR2a- and DR2b-presented peptides in the thymus, the amino acid preferences at deduced anchor positions for DR2a or DR2b (Figure 4C) were similar to peptides from EBV_B cells and MS brain tissues, but differences at other positions implied different peptide sources among these samples (Figures 1E and 2B). Indeed, DR2a-/DR2b-presented unique peptides and source proteins showed limited overlap between thymic tissues and primary_B cells/EBV_B cells/MS brain tissues (Figure S5A). Consistent with the central tolerance-inducing function of the thymus, the source proteins of the thymus-derived peptides are widely distributed in tissues of the human body (Figures 4D, S5B, and S5C). Detailed analyses of thymus-derived peptides revealed that neither $MBP_{(78–90)}$ nor $MBP_{(83–90)}$ was among the DR2a- and DR2b-presented immunopeptidomes. Except for $RGF1A_{(270–294)}$, we did not detect any peptides in the thymus from proteins that are specifically expressed in brain tissues (Figures 2D and 4E), suggesting that $CD4^+$ T cells recognizing $MBP_{(78–90)}$/$MBP_{(83–90)}$-$HLA\text{-}DR15$ complexes may not be deleted in the thymus and could be activated by EBV_B cells in the periphery.

Besides MS, EBV infection has been associated with other human autoimmune diseases such as rheumatoid arthritis (RA), systemic lupus erythematosus (SLE), ankylosing spondylitis (AS), and autoimmune hepatitis.[50,51] Interestingly, similar to $MBP_{(78–90)}$ and $MBP_{(83–90)}$ for MS, SLE-, and AS-associated autoantigen-derived peptides, DEK proto-oncogene $(DEK)_{(349–357)}$ and

(SI), and SI ≥ 2 was considered positive. 5–10 replicate wells for each condition of each sample, and the pooled data for all tested replicate wells are shown. Responses to the control CEF II peptide pool and anti-CD2/CD3/CD28 beads are shown at the bottom.

(B) 16 RRMS samples were divided into two groups: MBP peptide responsive ($n = 8$) and unresponsive ($n = 8$), and their respective data were pooled. Comparison of these two groups with respect to responses to the CEF II peptide pool that includes EBV-derived peptides.

(C) $CD45RA^-$ PBMCs from $HLA\text{-}DR15^+$ RRMS patients were labeled with CFSE and stimulated with pooled MBP peptides. After 7 days, cells were analyzed by flow cytometry. Proportions of memory $CD4^+$ T cells in the proliferating ($CFSE^{dim}$) and the highly proliferating ($CFSE^{low}$) compartments are shown in the pie charts.

(D) Proliferation of MBP peptide-responsive $CD45RA^-$ PBMCs from RRMS patients after stimulation with pooled MBP peptides for 7 days was detected by ^3H-thymidine incorporation assay in the presence of a blocking anti-HLA-DR antibody.

(E) $CD45RA^-$ PBMCs of $HLA\text{-}DR15^+$ RRMS patients were stimulated with pooled MBP peptides for 7 days. Concentrations of various Th subset-related cytokines in supernatants were detected by a bead-based immunoassay.

(F) CSF $CD4^+$ T cells from $HLA\text{-}DR15^+$ RRMS patients ($n = 3$) were co-cultured with irradiated autologous EBV_B cells as APCs and stimulated with the indicated MBP peptide pools. Proliferation of CSF $CD4^+$ T cells was analyzed on day 7.

(G) Immunofluorescence detection of EBV-infected B cells within meningeal tertiary lymphoid structures (TLSs) of two representative post-mortem MS cases (MS 402: I-III; MS 528: IV-VII): the expression of latent EBV nuclear antigen 2 (EBNA2, I, III, IV, and V), latent membrane protein 1 (LMP1 and VI), and major membrane antigen (glycoprotein gp250/350, VII) in meningeal $CD79a^+$ (I, II) or $CD19^+$ B cells (IV, VI, and VII), in particular within the core of meningeal TLS. Scale bar is 20 μm. Data are expressed as mean ± SEM, and p values were determined by unpaired t test.

See also Table S5.

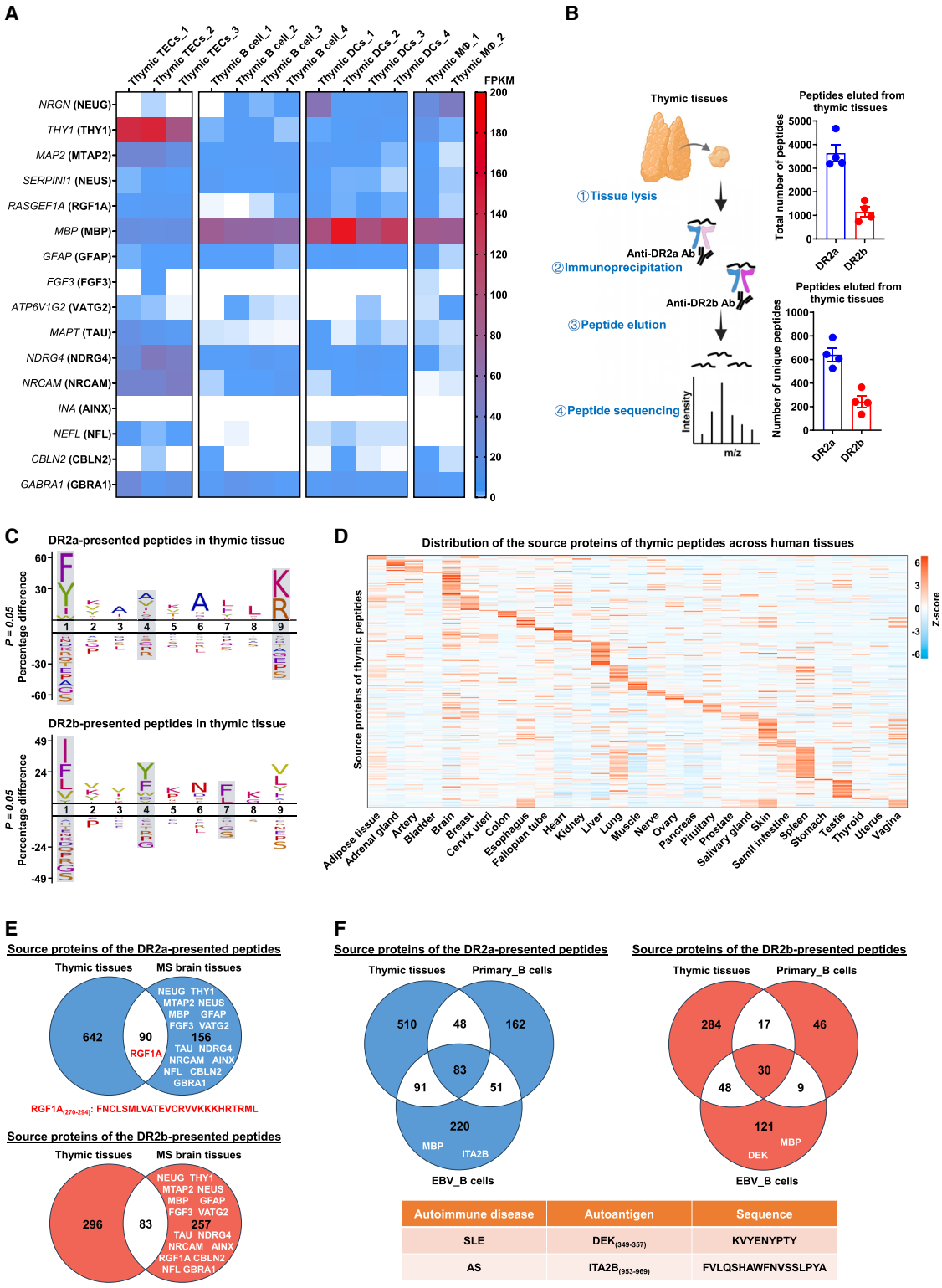

Autoimmune disease	Autoantigen	Sequence
SLE	DEK(349-357)	KVYENYPTY
AS	ITA2B(953-969)	FVLQSHAWFNVSSLPYA

Figure 4. MBP peptides were not detected in DR2a- and DR2b-presented peptidomes in thymic tissues

(A) Expression levels of peptides' source proteins specifically expressed in brain tissues in various APCs of thymic tissue.

(B) Workflow diagram for the identification of DR2a- and DR2b-presented peptides derived from human proteins in HLA-DR15^{+} thymic tissues. The total number of peptides and the number of unique peptides presented by DR2a and DR2b in thymic tissues are shown.

(legend continued on next page)

integrin alpha IIB (ITA2B)$_{(953–969)}$, could be eluted from EBV_B cells but not from thymic tissues or primary_B cells (Figure 4F), implying that EBV infection may also contribute to B cell presentation of peptides derived from other autoantigens and the development/perpetuation of SLE and AS.

Epitope recognition of HLA-DR15-presented MBP$_{(78–90)}$/MBP$_{(83–90)}$ on B cells differs from recognition of MBP$_{(83–99)}$

Myelin-specific CD4$^+$ T cells are considered important for the pathogenesis of MS,[52] and multiple pieces of evidence support the immunodominance of MBP$_{(83–99)}$,[53–61] along with its promiscuous binding to multiple HLA-DR molecules, including DR2a and DR2b.[62–64] Different from what we expected from prior data about the processing of MBP$_{(83–99)}$,[65] we did not find MBP$_{(83–99)}$ in the DR2a- and DR2b-presented immunopeptidomes from both EBV_B cells and MS brain tissues (Tables S2, S3, and S4). We had previously shown that binding to the HLA-DR15 molecules protects MBP$_{(83–99)}$ from cleavage.[65] Therefore, the fact that all peptides in this region were cleaved after the two F residues at positions 89 and 90 was highly surprising (Figure S4). Since MBP$_{(83–99)}$-specific CD4$^+$ T cell clones (TCCs) can recognize truncated versions of the MBP$_{(83–99)}$ peptide,[66] we wondered if MBP$_{(83–99)}$- and MBP$_{(78–90/83–90)}$-specific T cell recognition differed and tested two well-characterized MBP$_{(83–99)}$-specific autoreactive CD4$^+$ TCCs, TCC3A6, which is DR2a-restricted,[67] and TCC5F6, which is DR2b-restricted,[68] with the two shorter, naturally presented peptides. Neither TCC3A6 nor TCC5F6 responded to MBP$_{(78–90)}$ and MBP$_{(83–90)}$, and also not to MBP$_{(91–106)}$ and MBP$_{(91–114)}$ (Figure 5A), indicating that MBP$_{(78–90)}$ and MBP$_{(83–90)}$ represent CD4$^+$ T cell epitopes that are distinct from MBP$_{(83–99)}$, although they might have a common core epitope toward the N terminus. To examine this point further, we stimulated CD45RA$^-$ PBMCs from 4 RRMS patients with an MBP peptide pool including MBP$_{(78–90)}$, MBP$_{(83–90)}$, MBP$_{(91–106)}$, and MBP$_{(91–114)}$ to generate TCCs (Figure 5B). Memory CD4$^+$ T cells from all 4 samples responded to the MBP peptide pool, albeit with different strengths (Figure 5C). We then generated four CD4$^+$ TCCs from RRMS-2 and one each from RRMS-13, -17, and -18 (Figure 5D; Table S5). Consistent with the high levels of IFN-γ in the supernatant of CD45RA$^-$ PBMCs after MBP peptide pool stimulation (Figure 3E), all TCCs predominantly displayed a Th1 phenotype (Figure 5E). When assessing their fine specificity, all new CD4$^+$ TCCs responded strongly to MBP$_{(78–90)}$ and MBP$_{(83–90)}$ (Figure 5F), and none of the TCCs responded to the immunodominant MBP$_{(83–99)}$ and MOG$_{(35–55)}$ (Figure 5G). These data indicate that MBP$_{(78–90)}$ and MBP$_{(83–90)}$ are recognized differently from MBP$_{(83–99)}$ and represent two potential CD4$^+$ T cell autoantigens in MS. Since the responses to the C-terminal peptides, MBP$_{(91–106)}$ and MBP$_{(91–114)}$, were much weaker, we did not pursue these further.

Autoreactive CD4$^+$ T cells respond to MBP peptides ending with MBP$_{90}$ eluted from MS brain tissues

To examine HLA-DR15 as antigen-presenting molecules of the two MBP peptides in MS further, we tested the restriction of the MBP peptide-specific CD4$^+$ TCCs using a bare lymphocyte syndrome (BLS) B cell line expressing a single HLA-DR heterodimer, DR2a (BLS-DR2a cells) or DR2b (BLS-DR2b cells). CD4$^+$ TCCs responded to MBP$_{(78–90)}$ and/or MBP$_{(83–90)}$ when BLS-DR2a and/or BLS-DR2b cells were used as APCs (Figures 6A and 6B), in particular TCC 1642KA_TCC1B3, which responded strongly to both MBP$_{(78–90)}$ and MBP$_{(83–90)}$ presented by DR2b (Figures 6B and 6C). Testing TCCs with MBP peptides eluted from MS brain tissues surprisingly showed that the 1642KA_TCC1B3 responded to all MBP peptides ending at MBP$_{90}$ when BLS-DR2b cells but not BLS-DR2a cells were used as APCs. By contrast, MBP$_{(83–99)}$-specific TCCs, TCC3A6 and TCC5F6, did not respond to any of these (Figure 6D), suggesting that 1642KA_TCC1B3 differs from TCC3A6 and TCC5F6 and that the two F residues at positions 89 and 90 of MBP peptides ending at MBP$_{90}$ may be critical for 1642KA_TCC1B3 recognition. To clarify which amino acids in MBP$_{(83–90)}$ are involved in the interaction between the 1642KA_TCC1B3 TCR and the MBP$_{(83–90)}$/DR2b complex, we tested individual glycine-substituted peptides. V86, V87, or H88 substitution completely eliminated the T cell response, and F89 or F90 substitution reduced it (Figure 6E). N- and C-terminal truncations analysis disclosed that V86, H88, and F89 were critical amino acids (Figure 6F), together suggesting that the core epitope is VVHF. Structural predictions of the MBP$_{(83–90)}$/DR2a and MBP$_{(83–90)}$/DR2b complexes using AlphaFold3[69] identified VVHF as the main region for DR2a/DR2b binding and, interestingly, indicated that the MBP$_{(83–90)}$ peptide may bind to either allomorph in reverse orientation, albeit in different registers (Figure S6). However, coefficients of confidence slightly below 0.9 indicate that these structural predictions will need confirmation by other methods. In conclusion, these data support the importance of one or two F residues at positions 89 and 90 and that peripheral CD4$^+$ T cells that may have been activated by EBV infection-induced expression of MBP peptides respond to these not only in the peripheral immune system but also in the brain.

DISCUSSION

The HLA-DR15 haplotype and EBV play major roles as genetic and environmental risk factors for MS, respectively, and their effects are synergistic.[3] Several potential mechanisms of how

(C) 9 amino acid binding motifs of DR2a- and DR2b-presented peptides in thymic tissues.
(D) Distribution of the source proteins of both DR2a- and DR2b-presented thymic peptides across human tissues.
(E) Overlap of the source proteins of DR2a- and DR2b-presented peptides between thymic tissues and MS brain tissues. The distribution of source proteins specifically expressed in brain tissues is shown.
(F) Overlap of the source proteins of DR2a- and DR2b-presented peptides among thymic tissues, primary_B cells, and EBV_B cells. The source proteins that were identified as the autoantigens for various autoimmune diseases, and their peptides were only eluted from EBV_B cells, are shown.
Data are expressed as mean ± SEM.
See also Figure S5 and Table S6.

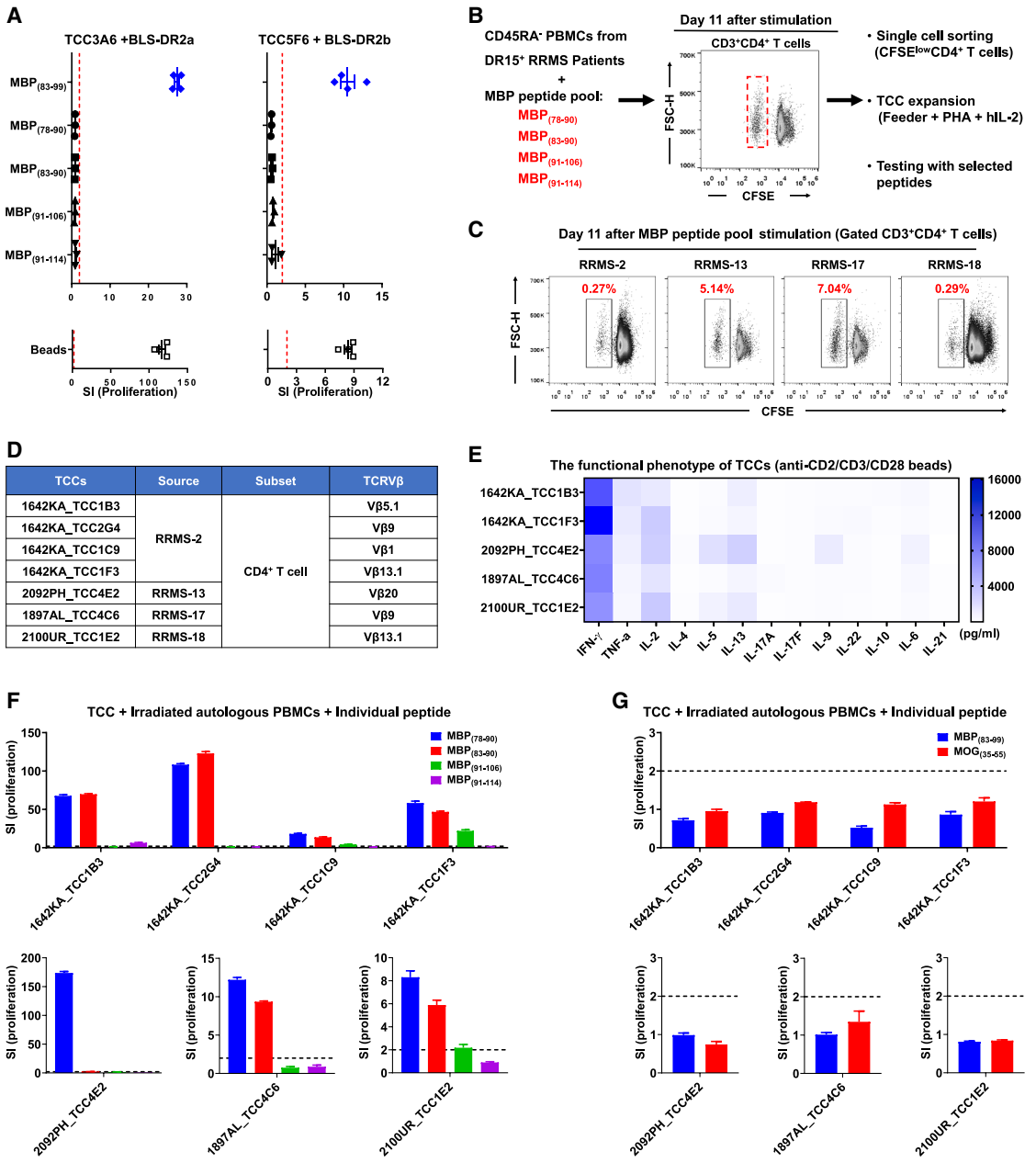

TCCs	Source	Subset	TCRVβ
1642KA_TCC1B3	RRMS-2	CD4+ T cell	Vβ5.1
1642KA_TCC2G4			Vβ9
1642KA_TCC1C9			Vβ1
1642KA_TCC1F3			Vβ13.1
2092PH_TCC4E2	RRMS-13		Vβ20
1897AL_TCC4C6	RRMS-17		Vβ9
2100UR_TCC1E2	RRMS-18		Vβ13.1

Figure 5. MBP peptide-specific CD4+ TCCs are identified in the PBMCs of HLA-DR15+ RRMS patients

(A) Proliferation of $MBP_{(83–99)}$-specific TCC3A6 and TCC5F6 after co-culture with irradiated BLS-DR2a or BLS-DR2b cells as APCs and stimulation with four MBP peptides eluted from EBV_B cells and cognate peptide $MBP_{(83–99)}$ for 3 days. Responses to anti-CD2/CD3/CD28 beads are shown at the bottom.

(B) Schematic depiction of how MBP peptide-specific $CD4^+$ TCCs were generated. CFSE-diluting $CD4^+$ T cells from $CD45RA^-$ PBMCs that had been stimulated with the pool of MBP peptides were isolated by single-cell sorting, then expanded with irradiated allogeneic PBMCs as feeders, phytohaemagglutinin (PHA), and human interleukin-2 (hIL-2), and finally assayed for specificity to individual MBP peptides.

(C–E) $CD45RA^-$ PBMCs from 4 HLA-$DR15^+$ RRMS patients were stimulated with pooled MBP peptides to generate TCCs. Proliferation of memory $CD4^+$ T cells was analyzed and sorted on day 11 by CFSE dilution (C). Seven new TCCs, which responded to pooled MBP peptides, were generated. Their corresponding source sample and TCRVβ type are shown in the table (D), and their cytokine secretion profile in (E).

(F) TCCs were co-cultured with irradiated autologous PBMCs as APCs and stimulated with individual MBP peptides. Proliferation was measured on day 3 by ^{3}H-thymidine incorporation assay.

(G) To assess if the TCCs also recognized $MBP_{(83–99)}$ and/or cross-recognized $MOG_{(35–55)}$. They were co-cultured with irradiated autologous PBMCs as APCs and stimulated with $MBP_{(83–99)}$ or $MOG_{(35–55)}$. Proliferation was measured on day 3 by ^{3}H-thymidine incorporation assay.

Data are expressed as mean ± SEM.

See also Table S5.

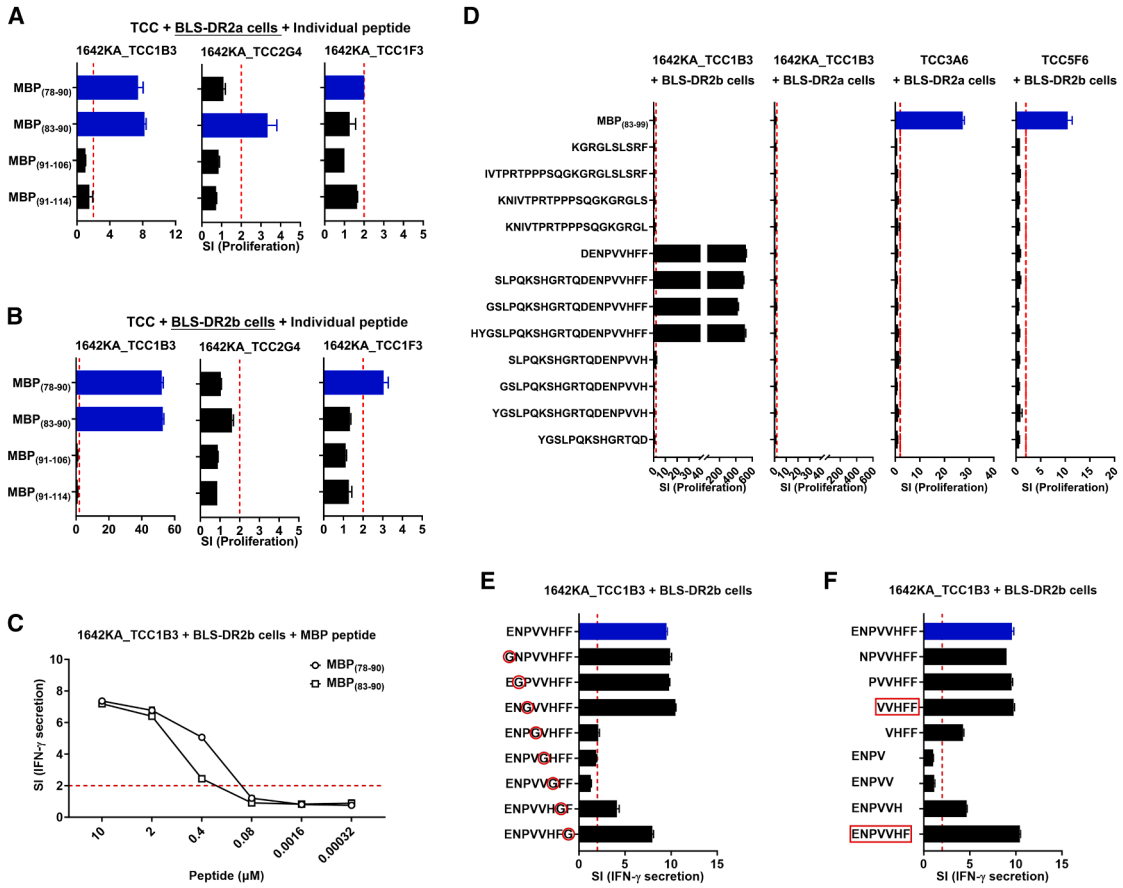

Figure 6. MBP peptide-specific CD4$^+$ TCCs highly respond to the whole MBP peptides ending at MBP$_{90}$ eluted from the MS brain tissues

(A and B) TCCs were co-cultured with irradiated BLS-DR2a (A) or BLS-DR2b cells as APCs (B) and stimulated with individual MBP peptides for 3 days. Proliferation of the TCCs was measured by ^{3}H-thymidine incorporation assay.

(C) Dose-response curves of 1642KA_TCC1B3 to MBP$_{(78–90)}$ and MBP$_{(83–90)}$ using irradiated BLS-DR2b cells as APCs. Reactivity of the TCCs was measured by IFN-γ ELISpot assay.

(D) 1642KA_TCC1B3, TCC3A6, and TCC5F6 were co-cultured with irradiated BLS-DR2a or BLS-DR2b cells as APCs and stimulated with MBP$_{(83–99)}$ and individual MBP peptides eluted from MS brain tissues for 3 days. Proliferation of the TCCs was measured by ^{3}H-thymidine incorporation assay.

(E) Response of 1642KA_TCC1B3 to glycine substitutions of the peptide MBP$_{(83–90)}$ using irradiated BLS-DR2b cells as APCs. Reactivity of the TCCs was measured by IFN-γ ELISpot assay.

(F) Response of 1642KA_TCC1B3 to N- and C-terminal truncations of the peptide MBP$_{(83–90)}$ using irradiated BLS-DR2b cells as APCs. Reactivity of the TCCs was measured by IFN-γ ELISpot assay.

Data are expressed as mean or mean ± SEM.

See also Figure S6.

EBV infection may be involved in MS have been reported,[6,9,70] and some of these mechanisms have been more pronounced or shown only in HLA-DR15$^+$ individuals, which indicates that the two risk factors interact functionally at multiple levels.

We recently analyzed the HLA-DR15-presented immunopeptidomes of primary B cells[10] with the assumption that peptides presented by HLA-DR15 molecules may drive the T/B cell autoproliferation that we found before.[39] We concluded that the weakly stimulatory HLA-DR15-derived peptides, which are presented on DR2a and DR2b, are likely involved in thymic selection and/or peripheral homeostatic maintenance of T cells that can be activated by certain pathogens, particularly EBV and *Akkermansia*, and are cross-reactive with MS autoantigens such as RASGRP2.[39] These findings prompted us to analyze the immunopeptidome of HLA-DR15$^+$ EBV-infected B cells in this study.

Following the above hypothesis, we examined the HLA-DR15-presented immunopeptidomes of EBV_B cells to demonstrate a potential mechanistic link between EBV infection, B cell antigen presentation, and the development of MS. We found that the transcriptomes and immunopeptidomes of EBV_B cells are altered compared with primary_B cells, and, most unexpectedly, that four MBP peptides are presented by EBV_B cells. The same three peptides were also identified among a much broader range of MBP peptides in highly inflamed MS brain tissue of HLA-DR15$^+$ MS patients but not in thymic tissues of HLA-DR15$^+$ HDs. Memory CD4$^+$ T cells from HLA-DR15$^+$ MS patients respond to these MBP peptides, while the responses of HDs

were much lower. Furthermore, CSF-infiltrating $CD4^+$ T cells also respond to these peptides. We then generated DR2a- or/and DR2b-restricted MBP peptide-specific TCCs from MS patients and tested these against both the MBP peptides ending at MBP_{90} and also the immunodominant $MBP_{(83–99)}$ that we and others had described a long time ago.[53–55,62,63,65,71] The results indicate that MBP peptides ending at MBP_{90} are recognized differently than $MBP_{(83–99)}$ and represent potential $CD4^+$ T cell autoantigens in MS. These data identify a novel mechanism of how EBV infection may contribute to MS pathogenesis in conjunction with the HLA-DR15 haplotype.

As described above, the relevance of $MBP_{(83–99)}$ with MS is supported by a wealth of data, including the development of spontaneous experimental autoimmune encephalomyelitis (EAE) in humanized transgenic mice expressing $MBP_{(83–99)}$-specific TCRs that are restricted by either DR2b or DR2a,[53,54] the increased immune reactivity in MS patients,[52] and the fact that it is a promiscuous binder to multiple HLA-DR molecules and recognized by $CD4^+$ T cells in the context of multiple HLA-DR alleles.[55,59] Further evidence is the demonstration of $MBP_{(85–99)}$/HLA-DR15 complexes as well as of $MBP_{(83–97)}$-specific autoantibodies existing in MS brain tissues.[61,72] By contrast, the DR2a- or DR2b-presented immunopeptidome data from both EBV_B cells and MS brain tissue show that all peptides in the immunodominant region of $MBP_{(83–99)}$ end at F90, indicating proteolytic cleavage at this amino acid. Potential explanations for the unexpected discrepancy are the following: it is important to note that the immunopeptidomics methodology had not been employed in the past. Furthermore, it is possible that the relatively low sensitivity of the method prevented the detection of $MBP_{(83–99)}$ or other peptides in this region that span F90-K91. The broader set of MBP peptides that are presented in MS brain tissue end with several different amino acids, i.e., p34(D), p39(D), p44(F), p46(G), p47(G), p48(D), p69(Y), p75(K), p68(G), p82(D), p88(H), p90(F), p116(G), p119(S), p124(F), p145(K), p149(K), p152(K), p166(P), p168(A), and p170(R) (last amino acid), suggesting cleavage by different proteases, but no peptide in our dataset spans amino acids F90 and K91.

To address if $MBP_{(78–90)}$/$MBP_{(83–90)}$-specific T cells also recognize $MBP_{(83–99)}$, we established TCCs that are restricted by either DR2a or DR2b and tested these with both peptides. $MBP_{(78–90)}$/$MBP_{(83–90)}$-specific T cells did not recognize $MBP_{(83–99)}$, hinting at distinct epitopes of the two types of autoreactive T cells, although this had already been indicated by the fact that F90 is at the C-terminal end of the $MBP_{(78–90)}$/$MBP_{(83–90)}$, while it is positioned in pockets I (N-terminal end) or IV (middle of the peptide binding groove) in $MBP_{(83–99)}$ in the context of binding to DR2a and DR2b, respectively. Previously, we had shown that a truncated version of a superagonist peptide of $MBP_{(83–99)}$, i.e., VIIFF derived from VIIFFKNVVIK, was recognized by TCC5F6, an $MBP_{(83–99)}$-specific, DR2b-restricted TCC,[66] but this sequence varies substantially from the VVHFF in the natural $MBP_{(83–99)}$ sequence.

A recent study reported that MBP peptides contained within the $MBP_{(158–195)}$ region were eluted from MHC class II molecules in mouse brain tissues, and they were able to induce suppressor $CD4^+$ T cells and thereby prevent CNS autoimmunity.[73] Interestingly, similar peptides, which were contained within the $MBP_{(26–50)}$ region of the main MBP isoform described in our study, were also eluted from HLA-DR15 molecules in human MS brain tissues. However, we do not know whether these and other peptides in our study may be capable of inducing suppressor/regulatory $CD4^+$ T cells. These sequences have not been found in the immunopeptidomes of EBV_B cells, and therefore, we currently cannot speculate about their role in humans.

Several conclusions can be drawn from our study. $MBP_{(78–90)}$/$MBP_{(83–90)}$ are potential MS autoantigens, possibly with a single core epitope, that result from EBV-induced processing alterations and are naturally presented on the MS-associated HLA-DR15 molecules of both EBV_B cells and highly inflamed MS brain tissue. In the context of MS pathogenesis, it suggests that not only RASGRP2, which is expressed by memory B cells,[39] but also $MBP_{(78–90)}$/$MBP_{(83–90)}$ are autoantigens that do not require molecular mimicry, i.e., similarity to foreign antigens, because they are both expressed by cells of the peripheral immune and the CNS. While we did not examine the MBP peptides starting with K91 in more detail, it is interesting that peptide 1–13 from the U24 protein of another MS-associated herpes virus, HHV6, shows a stretch of six amino acids (MDRPRTPPPSYSE; indicated in italics) with complete homology with $MBP_{(91–106)}$ KNIVTPRTPPPSQGKG.[74] In this case, molecular mimicry is likely the mechanism inducing T cell reactivity against the MBP peptide. Hence, both molecular mimicry and also expression of the same MS autoantigen in peripheral immune cells and the MS brain may contribute to starting and perpetuating the autoimmune response in MS, which adds an interesting new facet to our understanding of how the most important environmental and genetic risk factors of MS, i.e., EBV and HLA-DR15, may jointly contribute to MS pathogenesis. These findings should also be examined in other autoimmune diseases with a strong link to EBV, like RA and SLE.

Limitations of the study

While we provide a new mechanism for how EBV infection and the HLA-DR15 haplotype contribute jointly to MS, several limitations warrant further exploration. Whether the MBP peptides from the immunopeptidomes of EBV_B cells and MS brain tissue are more important than the long-known $MBP_{(83–99)}$ will need further studies as well as a more detailed analysis of the EBV-induced processing alterations in EBV_B cells. Also, the low sensitivity of the immunopeptidomics methodology may be the reason for not detecting the $MBP_{(83–99)}$ in the EBV_B cell- and MS brain immunopeptidomes and does not allow with certainty to exclude that the here-described MBP peptides are presented in the thymus. In addition, due to the lack of serum/plasma samples, we were unable to assess the EBV serostatus of all individuals.

RESOURCE AVAILABILITY

Lead contact

Further information and requests for resources and reagents should be directed to and will be fulfilled by the lead contact, Roland Martin (roland.martin@uzh.ch).

Materials availability

Reagents are available on request from the lead contact with a completed materials transfer agreement. Information on reagents used in this study is available in the key resources table.

Data and code availability

The RNA sequencing (RNA-seq) raw data have been deposited to the European Nucleotide Archive (ENA; https://www.ebi.ac.uk/ena/browser/home) with the accession code PRJEB34209[10] and the NCBI BioProject database (https://www.ncbi.nlm.nih.gov/bioproject/) with the accession code PRJNA1337418. The raw proteomics and immunopeptidomics data have been deposited to the ProteomeXchange Consortium via the PRIDE[75] partner repository with the dataset identifiers PXD068927 and PXD068488, respectively.

ACKNOWLEDGMENTS

Study support came from a European Research Council grant (ERC-2013-ADG 340733), the Clinical Research Priority Program MS (CRPP^{MS}), the University of Zurich, the Strategic Priority Research Program, the Chinese Academy of Sciences (#XDB0940303 and #XDB0490301), the National Key Research and Development Program of China (#2022YFC2304102), the Natural Science Foundation of China (#82271827, #32470954, #82471757, #92469102, and #32300747), the Institute of Health and Medicine, the Hefei Comprehensive National Science Center (#DJK-LX-2022005 and #2022KYQD010), and the Fundamental Research Funds for the Central Universities (#WK3520000016). Additional support came from Deutsche Forschungsgemeinschaft under Germany's Excellence Strategy (grant EXC2180-390900677 [J. Walz and H.-G.R.]), the German Cancer Consortium (DKTK [J. Walz and H.-G.R.]), Deutsche Forschungsgemeinschaft (DFG grant WA4608/1-2 [J. Walz]), Deutsche Krebshilfe (German Cancer Aid, 70114948 [J. Walz]), InvestBW (BW1_4064/03 [J. Walz]), Carl Zeiss Stiftung (P2024-02-012 [J. Walz]), Ernst Jung Prize for Medicine (H.-G.R.), Landesforschungspreis of Baden-Württemberg (H.-G.R.), INCa-DGOS-Inserm-ITMO Cancer_18000, and the European Union's Horizon Europe Research and Innovation Actions under grant no. 101137235 (BEHIND-MS) to R. Magliozzi. We thank C. Münz (Institute of Experimental Immunology, University of Zurich) for critically reading the manuscript and advice regarding the processing of MBP in EBV-infected B cells, R. Mariuzza (University of Maryland) for interpreting the structural predictions, U. Schanz and A. Müller (Hematology Clinic, University Hospital Zurich) for leukaphereses, T. Eng (NIMS) for contacting patients, D. Gveric (UK MS Brain Bank, London) for brain tissue, and patients for donating blood samples. This work was partially carried out at the Instruments Center for Physical Science, the University of Science and Technology of China, and the Instrument Sharing Center of the Institute of Health and Medicine, Hefei Comprehensive National Science Center.

AUTHOR CONTRIBUTIONS

J. Wang designed the overall study together with R. Martin; performed, analyzed, and interpreted experiments; and wrote the manuscript. Y.Q., Z.M., and F.L. designed, performed, and analyzed experiments; performed statistical analyses; and contributed to interpreting the data and revising the manuscript. M.W., L.M., J.B., H.-G.R., and J. Walz performed immunopeptidome isolation and sequence analyses; P.O. analyzed and interpreted transcriptome, proteomics, and immunopeptidomics experiments; L.J., H.Z., W.X., T.L., and W.F. collected samples, performed and analyzed experiments, and performed statistical analyses; Y.L. did tissue-specific gene enrichment analysis; J.T.N. and J.-H.L. generated allele-specific monoclonal antibodies; V.H. and M.H.-H. collected thymic tissues for immunopeptidome analysis and isolated thymic APCs for RNA-seq; B.R. co-designed, performed, and analyzed the proteomics experiments; F.M. performed the *in silico* structural predictions and contributed to the analysis of truncation and substitution variants of MBP$_{(78–90 \text{ and } 83–90)}$; M.S. generated and provided CSF-derived CD4$^+$ T cells for specificity testing; R. Magliozzi performed EBV-detection analyses in MS brain tissue. R.R. characterized and provided brain tissue for immunopeptidome analyses; R. Martin designed the overall study and experiments, supervised it, interpreted the data, and wrote the manuscript.

DECLARATION OF INTERESTS

R. Martin received remuneration for advisory roles and lectures for Roche, Novartis, Biogen, Merck, Genzyme, Neuway, CellProtect, Third Rock, Teva, and Swiss Rockets; is listed as an inventor on an NIH-held patent of daclizumab in MS and University of Zurich-held patents on JCV VP1 for vaccination against PML, JCV-specific neutralizing antibodies to treat PML, antigen-specific tolerization with peptide-coupled cells and novel autoantigens in MS, the use of designer neoantigens for glioblastoma (inventor R. Martin), and of peptides and TCRs shown in this study for the personalized treatment of glioblastoma (inventors Reza Naghavian, J. Wang, and R. Martin); and is a co-founder of Abata and a co-founder and employee of Cellerys AG.

STAR★METHODS

Detailed methods are provided in the online version of this paper and include the following:

- KEY RESOURCES TABLE
- EXPERIMENTAL MODEL AND SUBJECT DETAILS
  - Human subjects
  - Cell lines
  - Primary Cells
- METHOD DETAILS
  - EBV-transformed B cell line generation
  - Immunopeptidome isolation and analysis
  - Immunofluorescence
  - RNA Extraction, cDNA Synthesis, and PCR Analysis
  - Isolation of various antigen-presenting cells (APCs) from thymic tissues
  - RNA extraction and sequencing
  - Western blotting
  - Proteomic analysis
  - Tissue-specific gene enrichment analysis
  - Proliferation assay
  - Cytokine measurements
  - Flow cytometric analysis
  - T cell cloning and identification
- STATISTICAL ANALYSIS

SUPPLEMENTAL INFORMATION

Supplemental information can be found online at https://doi.org/10.1016/j.cell.2025.12.046.

Received: January 30, 2025
Revised: August 15, 2025
Accepted: December 20, 2025
Published: January 13, 2026

REFERENCES

1. Sospedra, M., and Martin, R. (2005). Immunology of multiple sclerosis. Annu. Rev. Immunol. *23*, 683–747. https://doi.org/10.1146/annurev.immunol.23.021704.115707.
2. Reich, D.S., Lucchinetti, C.F., and Calabresi, P.A. (2018). Multiple Sclerosis. N. Engl. J. Med. *378*, 169–180. https://doi.org/10.1056/NEJMra1401483.
3. Olsson, T., Barcellos, L.F., and Alfredsson, L. (2017). Interactions between genetic, lifestyle and environmental risk factors for multiple sclerosis. Nat. Rev. Neurol. *13*, 25–36. https://doi.org/10.1038/nrneurol.2016.187.
4. International Multiple Sclerosis Genetics Consortium. Electronic address: chris.cotsapas@yale.edu; International Multiple Sclerosis Genetics Consortium (2018). Low frequency and rare-coding variation contributes

to multiple sclerosis risk. Cell *175*, 1679–1687.e7. https://doi.org/10.1016/j.cell.2018.09.049.

5. Bjornevik, K., Cortese, M., Healy, B.C., Kuhle, J., Mina, M.J., Leng, Y., Elledge, S.J., Niebuhr, D.W., Scher, A.I., Munger, K.L., et al. (2022). Longitudinal analysis reveals high prevalence of Epstein-Barr virus associated with multiple sclerosis. Science *375*, 296–301. https://doi.org/10.1126/science.abj8222.
6. Soldan, S.S., and Lieberman, P.M. (2023). Epstein-Barr virus and multiple sclerosis. Nat. Rev. Microbiol. *21*, 51–64. https://doi.org/10.1038/s41579-022-00770-5.
7. Robinson, W.H., and Steinman, L. (2022). Epstein-Barr virus and multiple sclerosis. Science *375*, 264–265. https://doi.org/10.1126/science.abm7930.
8. Taylor, G.S., Long, H.M., Brooks, J.M., Rickinson, A.B., and Hislop, A.D. (2015). The immunology of Epstein-Barr virus-induced disease. Annu. Rev. Immunol. *33*, 787–821. https://doi.org/10.1146/annurev-immunol-032414-112326.
9. Münz, C. (2025). Epstein-Barr virus pathogenesis and emerging control strategies. Nat. Rev. Microbiol. *23*, 667–679. https://doi.org/10.1038/s41579-025-01181-y.
10. Wang, J., Jelcic, I., Mühlenbruch, L., Haunerdinger, V., Toussaint, N.C., Zhao, Y., Cruciani, C., Faigle, W., Naghavian, R., Foege, M., et al. (2020). HLA-DR15 Molecules Jointly Shape an Autoreactive T Cell Repertoire in Multiple Sclerosis. Cell *183*, 1264–1281.e20. https://doi.org/10.1016/j.cell.2020.09.054.
11. Lünemann, J.D., Jelcić, I., Roberts, S., Lutterotti, A., Tackenberg, B., Martin, R., and Münz, C. (2008). EBNA1-specific T cells from patients with multiple sclerosis cross react with myelin antigens and co-produce IFN-γ and IL-2. J. Exp. Med. *205*, 1763–1773. https://doi.org/10.1084/jem.20072397.
12. Wucherpfennig, K.W., and Strominger, J.L. (1995). Molecular mimicry in T cell-mediated autoimmunity: viral peptides activate human T cell clones specific for myelin basic protein. Cell *80*, 695–705. https://doi.org/10.1016/0092-8674(95)90348-8.
13. Tengvall, K., Huang, J., Hellström, C., Kammer, P., Biström, M., Ayoglu, B., Lima Bomfim, I., Stridh, P., Butt, J., Brenner, N., et al. (2019). Molecular mimicry between Anoctamin 2 and Epstein-Barr virus nuclear antigen 1 associates with multiple sclerosis risk. Proc. Natl. Acad. Sci. USA *116*, 16955–16960. https://doi.org/10.1073/pnas.1902623116.
14. Lanz, T.V., Brewer, R.C., Ho, P.P., Moon, J.S., Jude, K.M., Fernandez, D., Fernandes, R.A., Gomez, A.M., Nadj, G.S., Bartley, C.M., et al. (2022). Clonally expanded B cells in multiple sclerosis bind EBV EBNA1 and GlialCAM. Nature *603*, 321–327. https://doi.org/10.1038/s41586-022-04432-7.
15. Thomas, O.G., Bronge, M., Tengvall, K., Akpinar, B., Nilsson, O.B., Holmgren, E., Hessa, T., Gafvelin, G., Khademi, M., Alfredsson, L., et al. (2023). Cross-reactive EBNA1 immunity targets alpha-crystallin B and is associated with multiple sclerosis. Sci. Adv. *9*, eadg3032. https://doi.org/10.1126/sciadv.adg3032.
16. Marti, Z., Ruder, J., Thomas, O.G., Bronge, M., De La Parra Soto, L., Grönlund, H., Olsson, T., and Martin, R. (2024). Enhanced and cross-reactive in vitro memory B cell response against Epstein-Barr virus nuclear antigen 1 in multiple sclerosis. Front. Immunol. *15*, 1334720. https://doi.org/10.3389/fimmu.2024.1334720.
17. Sattarnezhad, N., Kockum, I., Thomas, O.G., Liu, Y., Ho, P.P., Barrett, A.K., Comanescu, A.I., Wijeratne, T.U., Utz, P.J., Alfredsson, L., et al. (2025). Antibody reactivity against EBNA1 and GlialCAM differentiates multiple sclerosis patients from healthy controls. Proc. Natl. Acad. Sci. USA *122*, e2424986122. https://doi.org/10.1073/pnas.2424986122.
18. Mrozek-Gorska, P., Buschle, A., Pich, D., Schwarzmayr, T., Fechtner, R., Scialdone, A., and Hammerschmidt, W. (2019). Epstein-Barr virus reprograms human B lymphocytes immediately in the prelatent phase of infection. Proc. Natl. Acad. Sci. USA *116*, 16046–16055. https://doi.org/10.1073/pnas.1901314116.
19. Küppers, R. (2003). B cells under influence: transformation of B cells by Epstein-Barr virus. Nat. Rev. Immunol. *3*, 801–812. https://doi.org/10.1038/nri1201.
20. Harley, J.B., Chen, X., Pujato, M., Miller, D., Maddox, A., Forney, C., Magnusen, A.F., Lynch, A., Chetal, K., Yukawa, M., et al. (2018). Transcription factors operate across disease loci, with EBNA2 implicated in autoimmunity. Nat. Genet. *50*, 699–707. https://doi.org/10.1038/s41588-018-0102-3.
21. Soldan, S.S., Su, C., Lamontagne, R.J., Grams, N., Lu, F., Zhang, Y., Gesualdi, J.D., Frase, D.M., Tolvinski, L.E., Martin, K., et al. (2021). Epigenetic Plasticity Enables CNS-Trafficking of EBV-infected B Lymphocytes. PLoS Pathog. *17*, e1009618. https://doi.org/10.1371/journal.ppat.1009618.
22. Lünemann, J.D., Kamradt, T., Martin, R., and Münz, C. (2007). Epstein-barr virus: environmental trigger of multiple sclerosis? J. Virol. *81*, 6777–6784. https://doi.org/10.1128/JVI.00153-07.
23. SoRelle, E.D., Reinoso-Vizcaino, N.M., Horn, G.Q., and Luftig, M.A. (2022). Epstein-Barr virus perpetuates B cell germinal center dynamics and generation of autoimmune-associated phenotypes in vitro. Front. Immunol. *13*, 1001145. https://doi.org/10.3389/fimmu.2022.1001145.
24. Läderach, F., Piteros, I., Fennell, É., Bremer, E., Last, M., Schmid, S., Rieble, L., Campbell, C., Ludwig-Portugall, I., Bornemann, L., et al. (2025). EBV induces CNS homing of B cells attracting inflammatory T cells. Nature *646*, 171–179. https://doi.org/10.1038/s41586-025-09378-0.
25. Oksenberg, J.R., Baranzini, S.E., Sawcer, S., and Hauser, S.L. (2008). The genetics of multiple sclerosis: SNPs to pathways to pathogenesis. Nat. Rev. Genet. *9*, 516–526. https://doi.org/10.1038/nrg2395.
26. Martin, R., Sospedra, M., Eiermann, T., and Olsson, T. (2021). Multiple sclerosis: doubling down on MHC. Trends Genet. *37*, 784–797. https://doi.org/10.1016/j.tig.2021.04.012.
27. Moutsianas, L., Jostins, L., Beecham, A.H., Dilthey, A.T., Xifara, D.K., Ban, M., Shah, T.S., Patsopoulos, N.A., Alfredsson, L., Anderson, C.A., et al. (2015). Class II HLA interactions modulate genetic risk for multiple sclerosis. Nat. Genet. *47*, 1107–1113. https://doi.org/10.1038/ng.3395.
28. Ascherio, A., Munger, K.L., and Lünemann, J.D. (2012). The initiation and prevention of multiple sclerosis. Nat. Rev. Neurol. *8*, 602–612. https://doi.org/10.1038/nrneurol.2012.198.
29. Lünemann, J.D., and Ascherio, A. (2009). Immune responses to EBNA1 Biomarkers in MS? Neurology *73*, 13–14. https://doi.org/10.1212/WNL.0b013e3181aa2a5f.
30. Hedström, A.K., Huang, J., Michel, A., Butt, J., Brenner, N., Hillert, J., Waterboer, T., Kockum, I., Olsson, T., and Alfredsson, L. (2019). High Levels of Epstein-Barr Virus Nuclear Antigen-1-Specific Antibodies and Infectious Mononucleosis Act Both Independently and Synergistically to Increase Multiple Sclerosis Risk. Front. Neurol. *10*, 1368. https://doi.org/10.3389/fneur.2019.01368.
31. van Sechel, A.C., Bajramovic, J.J., van Stipdonk, M.J.B., Persoon-Deen, C., Geutskens, S.B., and van Noort, J.M. (1999). EBV-induced expression and HLA-DR-restricted presentation by human B cells of αB-crystallin, a candidate autoantigen in multiple sclerosis. J. Immunol. *162*, 129–135. https://doi.org/10.4049/jimmunol.162.1.129.
32. Wang, C., Li, D., Zhang, L., Jiang, S., Liang, J., Narita, Y., Hou, I., Zhong, Q., Zheng, Z., Xiao, H., et al. (2019). RNA Sequencing Analyses of Gene Expression during Epstein-Barr Virus Infection of Primary B Lymphocytes. J. Virol. *93*, e00226–e00219. https://doi.org/10.1128/JVI.00226-19.
33. Babcock, G.J., Decker, L.L., Volk, M., and Thorley-Lawson, D.A. (1998). EBV persistence in memory B cells in vivo. Immunity *9*, 395–404. https://doi.org/10.1016/S1074-7613(00)80622-6.
34. Zhao, B. (2023). Epstein-Barr Virus B Cell Growth Transformation: The Nuclear Events. Viruses *15*, 832. https://doi.org/10.3390/v15040832.
35. Afrasiabi, A., Parnell, G.P., Fewings, N., Schibeci, S.D., Basuki, M.A., Chandramohan, R., Zhou, Y., Taylor, B., Brown, D.A., Swaminathan, S., et al. (2019). Evidence from genome wide association studies implicates reduced control of Epstein-Barr virus infection in multiple sclerosis

susceptibility. Genome Med. *11*, 26. https://doi.org/10.1186/s13073-019-0640-z.

36. Joseph, A.M., Babcock, G.J., and Thorley-Lawson, D.A. (2000). Cells expressing the Epstein-Barr virus growth program are present in and restricted to the naive B-cell subset of healthy tonsils. J. Virol. *74*, 9964–9971. https://doi.org/10.1128/JVI.74.21.9964-9971.2000.

37. Tosato, G., and Cohen, J.I. (2007). Generation of Epstein-Barr Virus (EBV)-Immortalized B Cell Lines. Curr. Protoc. Immunol. *27*, 22–24.

38. van Noort, J.M., van Sechel, A.C., Bajramovic, J.J., el Ouagmiri, M., Polman, C.H., Lassmann, H., and Ravid, R. (1995). The small heat-shock protein alpha B-crystallin as candidate autoantigen in multiple sclerosis. Nature *375*, 798–801. https://doi.org/10.1038/375798a0.

39. Jelcic, I., Al Nimer, F., Wang, J., Lentsch, V., Planas, R., Jelcic, I., Madjovski, A., Ruhrmann, S., Faigle, W., Frauenknecht, K., et al. (2018). Memory B Cells Activate Brain-Homing, Autoreactive CD4+ T Cells in Multiple Sclerosis. Cell *175*, 85–100.e23. https://doi.org/10.1016/j.cell.2018.08.011.

40. Bronge, M., Högelin, K.A., Thomas, O.G., Ruhrmann, S., Carvalho-Queiroz, C., Nilsson, O.B., Kaiser, A., Zeitelhofer, M., Holmgren, E., Linnerbauer, M., et al. (2022). Identification of four novel T cell autoantigens and personal autoreactive profiles in multiple sclerosis. Sci. Adv. *8*, eabn1823. https://doi.org/10.1126/sciadv.abn1823.

41. Coux, O., Tanaka, K., and Goldberg, A.L. (1996). Structure and functions of the 20S and 26S proteasomes. Annu. Rev. Biochem. *65*, 801–847. https://doi.org/10.1146/annurev.bi.65.070196.004101.

42. Paludan, C., Schmid, D., Landthaler, M., Vockerodt, M., Kube, D., Tuschl, T., and Münz, C. (2005). Endogenous MHC class II processing of a viral nuclear antigen after autophagy. Science *307*, 593–596. https://doi.org/10.1126/science.1104904.

43. Valečka, J., Almeida, C.R., Su, B., Pierre, P., and Gatti, E. (2018). Autophagy and MHC-restricted antigen presentation. Mol. Immunol. *99*, 163–170. https://doi.org/10.1016/j.molimm.2018.05.009.

44. Molnarfi, N., Schulze-Topphoff, U., Weber, M.S., Patarroyo, J.C., Prod'homme, T., Varrin-Doyer, M., Shetty, A., Linington, C., Slavin, A.J., Hidalgo, J., et al. (2013). MHC class II-dependent B cell APC function is required for induction of CNS autoimmunity independent of myelin-specific antibodies. J. Exp. Med. *210*, 2921–2937. https://doi.org/10.1084/jem.20130699.

45. Jelcic, I., Naghavian, R., Fanaswala, I., Macnair, W., Esposito, C., Calini, D., Han, Y., Marti, Z., Raposo, C., Sarabia Del Castillo, J., et al. (2025). T-bet+ CXCR3+ B cells drive hyperreactive B-T cell interactions in multiple sclerosis. Cell Rep. Med. *6*, 102027. https://doi.org/10.1016/j.xcrm.2025.102027.

46. Cruciani, C., Puthenparampil, M., Tomas-Ojer, P., Jelcic, I., Docampo, M.J., Planas, R., Manogaran, P., Opfer, R., Wicki, C., Reindl, M., et al. (2021). T-Cell Specificity Influences Disease Heterogeneity in Multiple Sclerosis. Neurol. Neuroimmunol. Neuroinflamm. *8*, e1075. https://doi.org/10.1212/NXI.0000000000001075.

47. Kisielow, P., and Miazek, A. (1995). Positive selection of T cells: rescue from programmed cell death and differentiation require continual engagement of the T cell receptor. J. Exp. Med. *181*, 1975–1984. https://doi.org/10.1084/jem.181.6.1975.

48. Fritz, R.B., and Zhao, M.L. (1996). Thymic expression of myelin basic protein (MBP). Activation of MBP-specific T cells by thymic cells in the absence of exogenous MBP. J. Immunol. *157*, 5249–5253. https://doi.org/10.4049/jimmunol.157.12.5249.

49. Sospedra, M., Ferrer-Francesch, X., Domínguez, O., Juan, M., Foz-Sala, M., and Pujol-Borrell, R. (1998). Transcription of a broad range of self-antigens in human thymus suggests a role for central mechanisms in tolerance toward peripheral antigens. J. Immunol. *161*, 5918–5929. https://doi.org/10.4049/jimmunol.161.11.5918.

50. Robinson, W.H., Younis, S., Love, Z.Z., Steinman, L., and Lanz, T.V. (2024). Epstein-Barr virus as a potentiator of autoimmune diseases. Nat. Rev. Rheumatol. *20*, 729–740. https://doi.org/10.1038/s41584-024-01167-9.

51. Mori, S., Kohyama, M., Yasumizu, Y., Tada, A., Tanzawa, K., Shishido, T., Kishida, K., Jin, H., Nishide, M., Kawada, S., et al. (2024). Neoself-antigens are the primary target for autoreactive T cells in human lupus. Cell *187*, 6071–6087.e20. https://doi.org/10.1016/j.cell.2024.08.025.

52. Bielekova, B., Sung, M.H., Kadom, N., Simon, R., McFarland, H., and Martin, R. (2004). Expansion and functional relevance of high-avidity myelin-specific CD4+ T cells in multiple sclerosis. J. Immunol. *172*, 3893–3904. https://doi.org/10.4049/jimmunol.172.6.3893.

53. Quandt, J.A., Huh, J., Baig, M., Yao, K., Ito, N., Bryant, M., Kawamura, K., Pinilla, C., McFarland, H.F., Martin, R., et al. (2012). Myelin Basic Protein-Specific TCR/HLA-DRB5*01:01 Transgenic Mice Support the Etiologic Role of DRB5*01:01 in Multiple Sclerosis. J. Immunol. *189*, 2897–2908. https://doi.org/10.4049/jimmunol.1103087.

54. Madsen, L.S., Andersson, E.C., Jansson, L., Krogsgaard, M., Andersen, C.B., Engberg, J., Strominger, J.L., Svejgaard, A., Hjorth, J.P., Holmdahl, R., et al. (1999). A humanized model for multiple sclerosis using HLA-DR2 and a human T-cell receptor. Nat. Genet. *23*, 343–347. https://doi.org/10.1038/15525.

55. Valli, A., Sette, A., Kappos, L., Oseroff, C., Sidney, J., Miescher, G., Hochberger, M., Albert, E.D., and Adorini, L. (1993). Binding of Myelin Basic Protein Peptides to Human Histocompatibility Leukocyte Antigen Class II Molecules and Their Recognition by T Cells from Multiple Sclerosis Patients. J. Clin. Investig. *91*, 616–628. https://doi.org/10.1172/JCI116242.

56. Ota, K., Matsui, M., Milford, E.L., Mackin, G.A., Weiner, H.L., and Hafler, D.A. (1990). T-cell recognition of an immunodominant myelin basic protein epitope in multiple sclerosis. Nature *346*, 183–187. https://doi.org/10.1038/346183a0.

57. Wucherpfennig, K.W., Ota, K., Endo, N., Seidman, J.G., Rosenzweig, A., Weiner, H.L., and Hafler, D.A. (1990). Shared human T cell receptor V beta usage to immunodominant regions of myelin basic protein. Science *248*, 1016–1019. https://doi.org/10.1126/science.1693015.

58. Pette, M., Fujita, K., Kitze, B., Whitaker, J.N., Albert, E., Kappos, L., and Wekerle, H. (1990). Myelin basic protein-specific T lymphocyte lines from MS patients and healthy individuals. Neurology *40*, 1770–1776. https://doi.org/10.1212/WNL.40.11.1770.

59. Martin, R., Howell, M.D., Jaraquemada, D., Flerlage, M., Richert, J., Brostoff, S., Long, E.O., McFarlin, D.E., and McFarland, H.F. (1991). A myelin basic protein peptide is recognized by cytotoxic T cells in the context of four HLA-DR types associated with multiple sclerosis. J. Exp. Med. *173*, 19–24. https://doi.org/10.1084/jem.173.1.19.

60. Martin, R., Jaraquemada, D., Flerlage, M., Richert, J., Whitaker, J., Long, E.O., McFarlin, D.E., and McFarland, H.F. (1990). Fine specificity and HLA restriction of myelin basic protein-specific cytotoxic T cell lines from multiple sclerosis patients and healthy individuals. J. Immunol. *145*, 540–548. https://doi.org/10.4049/jimmunol.145.2.540.

61. Krogsgaard, M., Wucherpfennig, K.W., Cannella, B., Hansen, B.E., Svejgaard, A., Pyrdol, J., Ditzel, H., Raine, C., Engberg, J., and Fugger, L. (2000). Visualization of myelin basic protein (MBP) T cell epitopes in multiple sclerosis lesions using a monoclonal antibody specific for the human histocompatibility leukocyte antigen (HLA)-DR2-MBP 85–99 complex. J. Exp. Med. *191*, 1395–1412. https://doi.org/10.1084/jem.191.8.1395.

62. Li, Y.L., Li, H.M., Martin, R., and Mariuzza, R.A. (2000). Structural basis for the binding of an immunodominant peptide from myelin basic protein in different registers by two HLA-DR2 proteins. J. Mol. Biol. *304*, 177–188. https://doi.org/10.1006/jmbi.2000.4198.

63. Vogt, A.B., Kropshofer, H., Kalbacher, H., Kalbus, M., Rammensee, H.G., Coligan, J.E., and Martin, R. (1994). Ligand motifs of HLA-DRB5*0101 and DRB1*1501 molecules delineated from self-peptides. J. Immunol. *153*, 1665–1673. https://doi.org/10.4049/jimmunol.153.4.1665.

64. Smith, K.J., Pyrdol, J., Gauthier, L., Wiley, D.C., and Wucherpfennig, K.W. (1998). Crystal structure of HLA-DR2 (DRA*0101, DRB1*1501) complexed with a peptide from human myelin basic protein. J. Exp. Med. *188*, 1511–1520. https://doi.org/10.1084/jem.188.8.1511.

65. Vergelli, M., Kalbus, M., Rojo, S.C., Hemmer, B., Kalbacher, H., Tranquill, L., Beck, H., McFarland, H.F., De Mars, R., Long, E.O., et al. (1997). T cell response to myelin basic protein in the context of the multiple sclerosis-associated HLA-DR15 haplotype: peptide binding, immunodominance and effector functions of T cells. J. Neuroimmunol. *77*, 195–203. https://doi.org/10.1016/S0165-5728(97)00075-1.

66. Hemmer, B., Kondo, T., Gran, B., Pinilla, C., Cortese, I., Pascal, J., Tzou, A., McFarland, H.F., Houghten, R., and Martin, R. (2000). Minimal peptide length requirements for CD4(+) T cell clones–implications for molecular mimicry and T cell survival. Int. Immunol. *12*, 375–383. https://doi.org/10.1093/intimm/12.3.375.

67. Vergelli, M., Hemmer, B., Utz, U., Vogt, A., Kalbus, M., Tranquill, L., Conlon, P., Ling, N., Steinman, L., McFarland, H.F., et al. (1996). Differential activation of human autoreactive T cell clones by altered peptide ligands derived from myelin basic protein peptide (87–99). Eur. J. Immunol. *26*, 2624–2634. https://doi.org/10.1002/eji.1830261113.

68. Vergelli, M., Hemmer, B., Kalbus, M., Vogt, A.B., Ling, N., Conlon, P., Coligan, J.E., McFarland, H., and Martin, R. (1997). Modifications of peptide ligands enhancing T cell responsiveness imply large numbers of stimulatory ligands for autoreactive T cells. J. Immunol. *158*, 3746–3752. https://doi.org/10.4049/jimmunol.158.8.3746.

69. Abramson, J., Adler, J., Dunger, J., Evans, R., Green, T., Pritzel, A., Ronneberger, O., Willmore, L., Ballard, A.J., Bambrick, J., et al. (2024). Accurate structure prediction of biomolecular interactions with AlphaFold 3. Nature *630*, 493–500. https://doi.org/10.1038/s41586-024-07487-w.

70. Bjornevik, K., Münz, C., Cohen, J.I., and Ascherio, A. (2023). Epstein-Barr virus as a leading cause of multiple sclerosis: mechanisms and implications. Nat. Rev. Neurol. *19*, 160–171. https://doi.org/10.1038/s41582-023-00775-5.

71. Bielekova, B., Goodwin, B., Richert, N., Cortese, I., Kondo, T., Afshar, G., Gran, B., Eaton, J., Antel, J., Frank, J.A., et al. (2000). Encephalitogenic potential of the myelin basic protein peptide (amino acids 83–99) in multiple sclerosis: results of a phase II clinical trial with an altered peptide ligand. Nat. Med. *6*, 1167–1175. https://doi.org/10.1038/80516.

72. Wucherpfennig, K.W., Catz, I., Hausmann, S., Strominger, J.L., Steinman, L., and Warren, K.G. (1997). Recognition of the immunodominant myelin basic protein peptide by autoantibodies and HLA-DR2-restricted T cell clones from multiple sclerosis patients. Identity of key contact residues in the B-cell and T-cell epitopes. J. Clin. Investig. *100*, 1114–1122. https://doi.org/10.1172/JCI119622.

73. Kim, M.W., Gao, W., Lichti, C.F., Gu, X., Dykstra, T., Cao, J., Smirnov, I., Boskovic, P., Kleverov, D., Salvador, A.F.M., et al. (2025). Endogenous self-peptides guard immune privilege of the central nervous system. Nature *637*, 176–183. https://doi.org/10.1038/s41586-024-08279-y.

74. Tejada-Simon, M.V., Zang, Y.C.Q., Hong, J., Rivera, V.M., and Zhang, J.Z. (2003). Cross-reactivity with myelin basic protein and human herpesvirus-6 in multiple sclerosis. Ann. Neurol. *53*, 189–197. https://doi.org/10.1002/ana.10425.

75. Perez-Riverol, Y., Bandla, C., Kundu, D.J., Kamatchinathan, S., Bai, J., Hewapathirana, S., John, N.S., Prakash, A., Walzer, M., Wang, S., et al. (2025). The PRIDE database at 20 years: 2025 update. Nucleic Acids Res. *53*, D543–D553. https://doi.org/10.1093/nar/gkae1011.

76. Planas, R., Santos, R., Tomas-Ojer, P., Cruciani, C., Lutterotti, A., Faigle, W., Schaeren-Wiemers, N., Espejo, C., Eixarch, H., Pinilla, C., et al. (2018). GDP-l-fucose synthase is a CD4(+) T cell-specific autoantigen in DRB3. Sci. Transl. Med. *10*, eaat4301. https://doi.org/10.1126/scitranslmed.aat4301.

77. Jensen, K.K., Andreatta, M., Marcatili, P., Buus, S., Greenbaum, J.A., Yan, Z., Sette, A., Peters, B., and Nielsen, M. (2018). Improved methods for predicting peptide binding affinity to MHC class II molecules. Immunology *154*, 394–406. https://doi.org/10.1111/imm.12889.

78. Brochet, X., Lefranc, M.P., and Giudicelli, V. (2008). IMGT/V-QUEST: the highly customized and integrated system for IG and TR standardized V-J and V-D-J sequence analysis. Nucleic Acids Res. *36*, W503–W508. https://doi.org/10.1093/nar/gkn316.

79. Colaert, N., Helsens, K., Martens, L., Vandekerckhove, J., and Gevaert, K. (2009). Improved visualization of protein consensus sequences by iceLogo. Nat. Methods. *6*, 786–787. https://doi.org/10.1038/nmeth1109-786.

80. Jain, A., and Tuteja, G. (2019). TissueEnrich: Tissue-specific gene enrichment analysis. Bioinformatics *35*, 1966–1967. https://doi.org/10.1093/bioinformatics/bty890.

81. Uhlén, M., Fagerberg, L., Hallström, B.M., Lindskog, C., Oksvold, P., Mardinoglu, A., Sivertsson, Å., Kampf, C., Sjöstedt, E., Asplund, A., et al. (2015). Proteomics. Tissue-based map of the human proteome. Science *347*, 1260419. https://doi.org/10.1126/science.1260419.

82. Galili, T., O'Callaghan, A., Sidi, J., and Sievert, C. (2018). heatmaply: an R package for creating interactive cluster heatmaps for online publishing. Bioinformatics *34*, 1600–1602. https://doi.org/10.1093/bioinformatics/btx657.

83. Thompson, A.J., Banwell, B.L., Barkhof, F., Carroll, W.M., Coetzee, T., Comi, G., Correale, J., Fazekas, F., Filippi, M., Freedman, M.S., et al. (2018). Diagnosis of multiple sclerosis: 2017 revisions of the McDonald criteria. Lancet Neurol. *17*, 162–173. https://doi.org/10.1016/S1474-4422(17)30470-2.

84. Mechelli, R., Umeton, R., Bellucci, G., Bigi, R., Rinaldi, V., Angelini, D.F., Guerrera, G., Pignalosa, F.C., Ilari, S., Patrone, M., et al. (2025). A disease-specific convergence of host and Epstein-Barr virus genetics in multiple sclerosis. Proc. Natl. Acad. Sci. USA *122*, e2418783122. https://doi.org/10.1073/pnas.2418783122.

85. Chen, S., Zhou, Y., Chen, Y., and Gu, J. (2018). fastp: an ultra-fast all-in-one FASTQ preprocessor. Bioinformatics *34*, i884–i890. https://doi.org/10.1093/bioinformatics/bty560.

86. Bray, N.L., Pimentel, H., Melsted, P., and Pachter, L. (2016). Near-optimal probabilistic RNA-seq quantification. Nat. Biotechnol. *34*, 525–527. https://doi.org/10.1038/nbt.3519.

87. Robinson, M.D., McCarthy, D.J., and Smyth, G.K. (2010). edgeR: a Bioconductor package for differential expression analysis of digital gene expression data. Bioinformatics *26*, 139–140. https://doi.org/10.1093/bioinformatics/btp616.

88. Türker, C., Akal, F., and Schlapbach, R. (2011). Life sciences data and application integration with B-fabric. J. Integr. Bioinform. *8*, 159. https://doi.org/10.2390/biecoll-jib-2011-159.

89. Demichev, V., Messner, C.B., Vernardis, S.I., Lilley, K.S., and Ralser, M. (2020). DIA-NN: neural networks and interference correction enable deep proteome coverage in high throughput. Nat. Methods *17*, 41–44. https://doi.org/10.1038/s41592-019-0638-x.

90. Wolski, W.E., Nanni, P., Grossmann, J., d'Errico, M., Schlapbach, R., and Panse, C. (2023). prolfqua: A Comprehensive R-Package for Proteomics Differential Expression Analysis. J. Proteome Res. *22*, 1092–1104. https://doi.org/10.1021/acs.jproteome.2c00441.

91. Huber, W., von Heydebreck, A., Sültmann, H., Poustka, A., and Vingron, M. (2002). Variance stabilization applied to microarray data calibration and to the quantification of differential expression. Bioinformatics *18*, S96–S104. https://doi.org/10.1093/bioinformatics/18.suppl_1.S96.

92. GTEx Consortium (2015). Human genomics. The Genotype-Tissue Expression (GTEx) pilot analysis: multitissue gene regulation in humans. Science *348*, 648–660. https://doi.org/10.1126/science.1262110.

STAR★METHODS

KEY RESOURCES TABLE

REAGENT or RESOURCE	SOURCE	IDENTIFIER
Antibodies		
Purified DR2a allele-specific monoclonal antibody	Purchased under an agreement from One Lambda (Thermo Fisher Scientific)	N/A
Purified DR2b allele-specific monoclonal antibody	Purchased under an agreement from One Lambda (Thermo Fisher Scientific)	N/A
Alexa Fluor 488-conjugated DR2a-specific antibody	Purchased under an agreement from One Lambda (Thermo Fisher Scientific)	N/A
Alexa Fluor 647-conjugated DR2b-specific antibody	Purchased under an agreement from One Lambda (Thermo Fisher Scientific)	N/A
Pacific Blue anti-human CD4 antibody (clone OKT4)	Biolegend	Cat# 317429; RRID:AB_1595438
PerCP/Cy5.5 anti-human CD3 antibody (clone OKT3)	Biolegend	Cat# 317336; RRID:AB_2561628
PE/Cy7 anti-human CD14 Antibody (clone 63D3)	Biolegend	Cat# 367112; RRID:AB_2566714
Alexa Fluor® 700 anti-human CD19 Antibody (clone HIB19)	Biolegend	Cat# 302226; RRID:AB_493751
Pacific Blue™ anti-human CD8 Antibody (Clone SK1)	Biolegend	Cat# 344718; RRID:AB_10551438
Purified anti-human CD3 Antibody (clone OKT3)	Biolegend	Cat# 317302; RRID:AB_571927
APC anti-human CD45RA (clone HI100)	Biolegend	Cat# 304112; RRID:AB_314416
Alexa Fluor® 700 anti-human CD45 Antibody (clone 2D1)	Biolegend	Cat# 368514; RRID:AB_2566374
PerCP/Cyanine5.5 anti-human CD326 (EpCAM) Antibody (clone 9C4)	Biolegend	Cat# 324214; RRID:AB_2098808
APC/Fire™ 750 anti-human HLA-DR Antibody (clone L243)	Biolegend	Cat# 307658; RRID:AB_2572101
Brilliant Violet 605™ anti-mouse/human CD11b Antibody (clone M1/70)	Biolegend	Cat# 101237; RRID: AB_11126744
CD11c Antibody, anti-human, APC, REAfinity™ (clone REA618 | S-HCL-3)	Miltenyi Biotec	Cat# 130-113-584; RRID:AB_2726184
CD20 Antibody, anti-human, VioBlue® (clone LT20)	Miltenyi Biotec	Cat# 130-113-378; RRID:AB_2726146
PE anti-human HLA-DR Antibody (Clone L243)	Biolegend	Cat# 307606; RRID:AB_314684
Purified anti-human HLA-DR Antibody (Clone L243)	Provided by HG. Rammensee, University of Tubingen, Germany	N/A
TCR Vβ1-PE, BL37.2, 1 mL, ASR	Beckman Coulter	Cat# IM2355; RRID:AB_131329
TCR Vβ2-PE, MPB,2D5, 1 mL, ASR	Beckman Coulter	Cat# IM2213; RRID:AB_131311
TCR Vβ3-FITC, CH92, 1 mL, ASR	Beckman Coulter	Cat# IM2372; RRID:AB_131046
TCR Vβ5.1-FITC, IMMU 157, 1 mL, ASR	Beckman Coulter	Cat# IM1552; RRID:AB_131023
TCR Vβ5.2-FITC, 36213, 1 mL, ASR	Beckman Coulter	Cat# IM1482; RRID:AB_130872
TCR Vβ7.1-PE, ZOE, 1 mL, ASR	Beckman Coulter	Cat# IM2287; RRID:AB_131323
TCR Vβ8-FITC, 56C5.2, 1 mL, ASR	Beckman Coulter	Cat# IM1233; RRID:AB_130922
TCR Vβ9-PE, FIN9, 1 mL, ASR	Beckman Coulter	Cat# IM2003; RRID:AB_131193
TCR Vβ11-FITC, C21, 1 mL, ASR	Beckman Coulter	Cat# IM1586; RRID:AB_131027
TCR Vβ12-PE, VER2.32.1, 1 mL, ASR	Beckman Coulter	Cat# IM2291; RRID:AB_131198

(*Continued on next page*)

Continued

REAGENT or RESOURCE	SOURCE	IDENTIFIER
TCR Vβ13.1-PE, IMMU 222, 1 mL, ASR	Beckman Coulter	Cat# IM2292; RRID:AB_131326
TCR Vβ13.6-FITC, JU74.3, 1 mL, ASR	Beckman Coulter	Cat# IM1330; RRID:AB_131012
TCR Vβ14-PE, CAS1.1.3, 1 mL, ASR	Beckman Coulter	Cat# IM2047; RRID:AB_131304
TCR Vβ16-FITC, TAMAYA1.2, 1 mL, ASR	Beckman Coulter	Cat# IM1560; RRID:AB_130875
TCR Vβ17-FITC, E17.5F3.15.13, 1 mL, ASR	Beckman Coulter	Cat# IM1234; RRID:AB_131007
TCR Vβ18-PE, BA62.6, 1 mL, ASR	Beckman Coulter	Cat# IM2049; RRID:AB_131305
TCR Vβ20-PE, ELL1.4, 1 mL, ASR	Beckman Coulter	Cat# IM2295; RRID:AB_131328
TCR Vβ21.3-FITC, IG125, 1 mL, ASR	Beckman Coulter	Cat# IM1483; RRID:AB_131021
TCR Vβ22-FITC, IMMU 546, 1 mL, ASR	Beckman Coulter	Cat# IM1484; RRID:AB_131022
TCR Vβ23-PE, AF23, 1 mL, ASR	Beckman Coulter	Cat# IM2004; RRID:AB_131302
TCR Vβ5.3-PE, 3D11, 1 mL, ASR	Beckman Coulter	Cat# IM2002; RRID:AB_131230
Alpha Tubulin Monoclonal antibody (Clone 1E4C11)	Proteintech	Cat# 66031-1-Ig; RRID:AB_11042766
Purified anti-Myelin Basic Protein Antibody (Clone SMI 99)	Biolegend	Cat# 808403; RRID:AB_2734562
LC3A/B (D3U4C) XP® Rabbit mAb	Cell signaling technology	Cat# 12741; RRID:AB_2617131
PSMB8 Polyclonal antibody	Proteintech	Cat# 14859-1-AP; RRID:AB_2268923
Beta Actin Recombinant antibody	Proteintech	Cat# 81115-1-RR; RRID: AB_2923704
HRP-labeled Goat Anti-Rabbit IgG(H+L)	Beyotime	Cat# A0208; RRID: AB_2892644
HRP-labeled Goat Anti-Mouse IgG(H+L)	Beyotime	Cat# A0216; RRID: AB_2860575
Mouse Anti-EBNA2 Monoclonal Antibody, Unconjugated, Clone PE2	Abcam	Cat# ab90543; RRID: AB_2049594
EBV Latent Membrane Protein antibody [CS 1–4]	Abcam	Cat# ab78113; RRID: AB_1566182
Epstein Barr Virus gp250/350 Monoclonal Antibody (C61H)	Thermo Fisher Scientific	Cat# MA1-7272; RRID: AB_1017112
CD79A Antibody	Novus	Cat# NBP3-24725; RRID: AB_3634855
Recombinant Anti-CD19 antibody [EPR5906]	Abcam	Cat# ab134114; RRID: AB_2801636
Biological Samples		
Leukaphereses from MS patients	This paper	N/A
Buffy coats from HDs	This paper	N/A
PBMCs from HDs	MileCell Bio	N/A
Thymic tissues	This paper	N/A
MS brain tissues	This paper	N/A
Cerebrospinal fluid (CSF)	This paper, Planas et al.[76] and Cruciani et al.[46]	N/A
Chemicals, Peptides, and Recombinant Proteins		
Bovine serum albumin (BSA)	Roth	Cat# 3854.3
Carboxyfluorescein diacetate N-succinimidyl ester (CFSE)	Sigma-Aldrich	Cat# 21888
Dimethyl sulfoxide (DMSO)	Applichem	Cat# A3672
Ficoll	Eurobio	Cat# GAUFIC0065
EDTA solution pH 8.0 (0.5 M)	AppliChem	Cat# A3145,1000
L-glutamine	Thermo Fisher Scientific	Cat# 25030024
Penicillin-Streptomycin Solution, 100x	Corning	Cat# 30-002-CI
Gentamicin	Sigma-Aldrich	Cat# G1397
MEM Non-Essential Amino Acids Solution (100X)	Gibco	Cat# 11140050

(*Continued on next page*)

Continued

REAGENT or RESOURCE	SOURCE	IDENTIFIER
Sodium Pyruvate (100 mM)	Gibco	Cat# 11360070
2-Mercaptoethanol (50 mM)	Gibco	Cat# 31350010
Human IL-2 containing supernatant (produced with T6 cell line)	Provided by F. Sallusto, IRB, Bellinzona, Switzerland	N/A
LIVE/DEAD Fixable Aqua Dead Cell Stain Kit	Thermo Fisher Scientific	Cat# L34957
Methyl-^{3}H-thymidine	Hartmann Analytic	Cat# M1762
Peptides	Peptides&Elephants	This paper
Peptides	GL Biochem	This paper
Remel™ PHA Purified	Thermo Fisher Scientific	Cat# R30852801
QIAzol lysis reagent	QIAGEN	Cat# 79306
CEF II peptide pool	Peptides&Elephants	N/A
Phytohemagglutinin-L (PHA-L)	Sigma-Aldrich	Cat# L2769
Liberase™ TM Research Grade	Roche	Cat# 5401119001
DNase I, recombinant	Roche	Cat# 04536282001
CHAPS	PanReac AppliChem	Cat# A1099.0050
cOmplete™ Protease Inhibitor Cocktail	Roche	Cat# 11697498001
Trifluoroacetic acid (TFA)	Sigma-Aldrich	Cat# 299537
RIPA buffer	EpiZyme	Cat# PC101
Protease inhibitors cocktail	EpiZyme	Cat# GRF101
Pierce BCA Protein Assay Kit	Thermo Scientific	Cat# 23225
Immunoglobulin G from human serum	Sigma-Aldrich	Cat# 56834
RPMI-1640 medium	Sigma-Aldrich	Cat# R0883
IMDM medium	GE healthcare	Cat# SH30259.01
X-Vivo medium	Lonza	Cat# BE04-418F
Fetal calf serum (FCS)	Eurobio	Cat# CVFSVF0001
DAPI	Sigma-Aldrich	Cat# 28718-90-3
Human serum	Blood Bank Basel, Switzerland	N/A
Critical Commercial Assays		
CD45RA MicroBeads, human	Miltenyi Biotec	Cat# 130-045-901
CD19 MicroBeads, human	Miltenyi Biotec	Cat# 130-050-301; RRID: AB_2848166
CD4 MicroBeads, human	Miltenyi Biotec	Cat# 130-045-101; RRID:AB_2889919
LEGENDplex Human T Helper Cytokine Panels	Biolegend	Cat# 740001; RRID: AB_2784515
T Cell Activation/Expansion Kit, human	Miltenyi Biotec	Cat# 130-091-441
ELISpot Pro: Human IFN-γ (ALP)	Mabtech	Cat# 3420-2AST-10
RNeasy Mini Kit (50)	Qiagen	Cat# 74104
Total RNA Kit	Omega	Cat# R6834-01
Evo M-MLV Reverse Transcription Mix Kit	Accurate Biology	Cat# AG11728
2× TransStart Fast Pfu PCR Super Mix	TRANS	Cat# AS221
Cell Proliferation ELISA, BrdU (colorimetric)	Roche	Cat# 11647229001
Super Red	Biosharp	Cat# BS354B
Deposited Data		
RNA-seq raw data of various antigen-presenting cells (APCs) from thymic tissues	This paper	PRJEB34209
RNA-seq raw data of EBV_B cells	This paper	PRJNA1337418
Raw proteomics data	This paper	PXD068927
Raw immunopeptidomics data	This paper	PXD068488

(*Continued on next page*)

Continued

REAGENT or RESOURCE	SOURCE	IDENTIFIER
Experimental Models: Cell Lines		
BLS-DR2a cells	Generated by B. Kwok, Benaroya Research Institute, Seattle	N/A
BLS-DR2b cells	Generated by B. Kwok, Benaroya Research Institute, Seattle	N/A
TCC3A6	Vergelli et al.[67]	N/A
TCC5F6	Vergelli et al.[65,68]	N/A
Oligonucleotides		
Primer: *Goli-MBP* forward: 5′-ATGGGAAAC CACGCAGGCAAACGAGAAT-3′	Sangon Biotech	N/A
Primer: *MBP* forward: 5′-ATGGCGTCACAG AAGAGACCCTCC-3′	Sangon Biotech	N/A
Primer: Shared reverse primer for both *Goli-MBP* and *MBP*: 5′-CCAGAGCCC CGCTTGGGC-3′	Sangon Biotech	N/A
Software and Algorithms		
FlowJo	Tree Star	https://www.flowjo.com/; RRID: SCR_008520
GraphPad Prism 8.0	Graphpad	https://www.graphpad.com/; RRID: SCR_002798
NetMHCII 2.3 Server	Jensen et al.[77]	http://www.cbs.dtu.dk/services/NetMHCII-2.3/
Venny2.1	Oliveros, J.C. (2007-2015) Venny. An interactive tool for comparing lists with Venn's diagrams.	https://bioinfogp.cnb.csic.es/tools/venny/index.html; RRID:SCR_016561
IMGT/V-QUEST	Brochet et al.[78]	http://www.imgt.org/IMGT_vquest/vquest; RRID:SCR_010749
iceLogo	Colaert et al.[79]	https://iomics.ugent.be/icelogoserver/; RRID:SCR_012137
Wei Sheng Xin	Newcore Biotech	https://www.bioinformatics.com.cn/
CytoNavigator	NovelBio	https://sc.novelbrain.com/login
TissueEnrich	Jain and Tuteja[80]	https://tissueenrich.gdcb.iastate.edu/
Human Protein Atlas	Uhlen et al.[81]	http://www.proteinatlas.org/;RRID:SCR_006710
Heatmaply	Galili et al.[82]	https://heatmaply.com/
Biorender	BioRender	http://biorender.com; RRID:SCR_018361

EXPERIMENTAL MODEL AND SUBJECT DETAILS

Human subjects

Leukaphereses were collected from HLA-DR15$^+$ 16 RRMS patients for EBV-transformed B cell line generation (n = 3), HLA immunopeptidome analyses (n = 3), proliferation assays (n = 16), and T cell cloning (n = 4). Leukaphereses from MS patients were collected at the Hematology Clinic, University Hospital Zurich, Zurich, Switzerland. Buffy coats (n = 7) and PBMCs (n = 9) from HLA-DR15$^+$ HDs were acquired for proliferation assays from the Blutspende Zurich, Zurich, Switzerland and Milecell Biotechnology Inc. Shanghai, China. Thymic tissues from HLA-DR15$^+$ immunologically healthy children undergoing cardiac surgery were collected at the University Children's Hospital Zurich, Zurich, Switzerland (n = 4) for HLA immunopeptidome analyses (n = 4). Highly inflamed MS brain tissues were collected from the UK MS Society Tissue Bank, Imperial College London, London, UK for HLA immunopeptidome analyses (n = 4). MS was diagnosed according to the revised McDonald criteria.[83] The study was approved by the Biomedical Ethics Committee of University of Science and Technology of China (2022KY302) and the Cantonal Ethical Committee of Zurich, Switzerland (EC-No. of the research project 2013-0001, approved on 5th June 2013, and EC-No. of the ERC grant 2014-0699, approved on 27th February 2015).

Cell lines

BLS-DR2a and -DR2b cells are HLA class II-deficient B cell line transfected with the genes encoding DRA*01:01P/DRB5*01:01 (BLS-DR2a cells) or DRA*01:01P/ DRB1*15:01 (BLS-DR2b cells). TCC3A6 and TCC5F6 were generated from HLA-DR15$^+$ MS patients. TCC3A6 recognizes $MBP_{(83-99)}$ and is restricted by DR2a.[67] TCC5F6 is also $MBP_{(83-99)}$-specific but restricted by DR2b.[68] BLS-DR2a cell, BLS-DR2b cell, TCC3A6, and TCC5F6 were cultured as previously described.[10]

Primary Cells

PBMCs in leukaphereses or buffy coats were isolated using Ficoll (Eurobio, Les Ulis, France) density gradient centrifugation. Isolated PBMCs were cryopreserved in freezing medium containing 90% heat-inactivated FCS (Eurobio) and 10% dimethyl sulfoxide (DMSO; Applichem, Darmstadt, Germany) and stored in liquid nitrogen. CD4$^+$ T cells in the CSF of HLA-DR15$^+$ RRMS patients were purified by positive selection using CD4 microbeads, human (Miltenyi, Bergisch Gladbach, Germany) and then expanded as previously described.[46,76]

METHOD DETAILS

EBV-transformed B cell line generation

PBMCs from HLA-DR15$^+$ RRMS patients were added at 1×10^6 cells/ml in 5 ml RPMI-1640 complete medium (Sigma-Aldrich, Missouri, USA) containing 10% heat-inactivated FCS (Eurobio), 2mM L-glutamine (ThermoFisher Scientific, Waltham, USA), 100 U/ml penicillin (Corning, NY, USA), 100 μg/ml streptomycin (Corning), and 50 μg/mL gentamicin (Sigma-Aldrich) into 25 cm^2 cell culture flasks, and EBV supernatant and 1μg/ml anti-CD3 antibody (OKT3, Biolegend, San Diego, USA) were then added. The new RPMI-1640 complete medium was added when the medium turned yellow, and the cells were transferred to 75 cm^2 cell culture flasks if necessary. The expanded EBV-transformed B cell lines were harvested and cryopreserved for subsequent experiments.

Immunopeptidome isolation and analysis

For immunopeptidome isolation of primary_B cells (n = 3), cryopreserved PBMCs from HLA-DR15$^+$ donors were thawed and washed twice with X-VIVO 15™ medium (Lonza, Basel, Switzerland), and over 50 mio primary B cells were then purified by positive selection using CD19 microbeads, human (Miltenyi) and used for immunopeptidome analysis. For immunopeptidome isolation of EBV_B cells from MS patients (n = 3) and HDs (n = 4), cryopreserved cells were thawed and washed twice with PBS, and over 50 mio EBV_B cells were used for immunopeptidome analysis. For the thymic tissues (around 1 g) and highly inflamed MS brain tissues (around 4 g), immunopeptidomes were isolated directly using the frozen tissues. The isolation and analysis of the immunopeptidome presented by DR2a and DR2b in primary_B cells, EBV_B cells, MS brain tissues, and thymic tissues were conducted as previously described.[10]

Immunofluorescence

Immunofluorescence assessment of FFPE (7-μm-thick) brain sections obtained from 4 post-mortem MS cases (MS402, 432, 438 and 528) examined in the study, was performed for the detection of EBV antigens, including EBV nuclear antigen 2 (EBNA2), latent membrane protein 1 (LMP1), and the major membrane antigen (glycoprotein gp250/350). Antigen retrieval was performed in the steamer in citrate buffer (pH = 6) for 30 min for FFPE and 5 min for fixed-frozen tissues as previously optimized.[84] Sections were incubated for 1 h with 10% of normal donkey sera (NDS) and then with the primary antibodies (anti-EBNA2 antibody; anti-LMP antibody; anti-gp250/350 antibody; anti-CD79a antibody; anti-CD19 antibody) diluted in PBS containing 5% NDS, overnight at room temperature. Sections were incubated with the appropriate secondary antibody conjugated to a fluorochrome and the autofluorescence was removed with Sudan Black for 2 min. Nuclei counterstained with DAPI (Sigma-Aldrich). Sections were mounted with Vectashield Antifade Mounting Media (Vector Laboratories) and images were acquired using Olympus microscope (CBH CoolLED pE300).

RNA Extraction, cDNA Synthesis, and PCR Analysis

Total RNA was extracted from EBV_B cells and primary_B cells using the Total RNA Kit (Omega, Norcross, Georgia) according to the manufacturer's instructions. The isolated RNA was then reverse transcribed into cDNA using the Evo M-MLV Reverse Transcription Mix Kit (Accurate Biology, Changsha, China). The expression levels of *Goli-MBP* and *MBP* were analyzed by PCR using the 2× TransStart Fast Pfu PCR Super Mix (TRANS, Beijing, China). The primer sequences were as follows: *Goli-MBP* forward primer: 5′-ATGGGAAACCACGCAGGCAAACGAGAAT-3′; *MBP* forward primer: 5′-ATGGCGTCACAGAAGAGACCCTCC-3′; Shared reverse primer for both *Goli-MBP* and *MBP*: 5′-CCAGAGCCCCGCTTGGGC-3′. PCR cycling conditions were as follows: initial denaturation at 95 °C for 3 min; followed by 32 cycles of 95 °C for 30 s, 60 °C for 20 s, and 72 °C for 1 min; with a final extension at 72 °C for 10 min. *β-actin* (forward: 5′-TTGCCGACAGGATGCAGAA-3′; reverse: 5′-GCCGATCCACACGGAGTACTT-3′) served as the internal control. PCR products were separated by electrophoresis on a 1.5% agarose gel, stained with Super Red (Biosharp, Hefei, China), and imaged under UV light.

Isolation of various antigen-presenting cells (APCs) from thymic tissues

Thymic tissues were dissociated using 0.4 mg/ml Liberase™ (Roche, Basel, Switerland) and 20 μg/ml DNase I (Roche), and enriched APCs were prepared as previously described.[10] Enriched APCs were stained for surface markers using anti-human CD45 antibody, anti-human EpCAM antibody, anti-human HLA-DR antibody, anti-human CD11b antibody, anti-human CD11c antibody, and anti-human CD20 antibody (Biolegend). HLA-DR$^+$ TECs (EpCAM$^+$CD45$^-$HLA-DR$^{int\text{-}high}$), HLA-DR$^+$ B cells (CD20$^+$CD45$^+$HLA-DR$^{int\text{-}high}$), HLA-DR$^+$ DCs (CD11c$^+$CD45$^+$HLA-DR$^+$), and HLA-DR$^+$ macrophages (CD11b$^+$CD45$^+$HLA-DR^{int}) were sorted using a FACSAria III 4L (BD Biosciences) and resuspended in Qiazol (QIAGEN, Hilden, Germany) for RNA extraction.

RNA extraction and sequencing

Primary_B cells were purified by magnetic cell separation, and RNA from purified primary_B cells and EBV_B cells was extracted using the RNeasy Mini Kit (Qiagen, Hilden, Germany). RNA quality was assessed using a Qubit® 1.0 Fluorometer (Life Technologies, California, USA) and a Fragment Analyzer (Agilent, Santa Clara, California, USA). Only samples with a 260/280 ratio of 1.8–2.1 and a 28S/18S ratio of 1.5–2, and an RNA integrity number (RIN) $\geq$ 8 were processed. Two sets of RNA-seq libraries were generated: three paired primary_B cells and EBV_B cells from RRMS patients, and four EBV_B cells from HDs together with four EBV_B cells from RRMS patients. For both sets, 50–1000 ng of total RNA was poly(A)-enriched, reverse-transcribed into double-stranded cDNA, fragmented, end-repaired, ligated to adapters with unique dual indices (UDI), PCR-enriched, and quality-checked with a Qubit® Fluorometer and Fragment Analyzer. Libraries showed an average fragment size of ~260 bp and were normalized to 10 nM in Tris-Cl 10 mM, pH 8.5 with 0.1% Tween-20. Libraries from paired primary_B cells and EBV_B cells from RRMS patients were prepared with the TruSeq Stranded mRNA kit (Illumina) and sequenced on a NovaSeq 6000 with single-end 100 bp reads. Libraries from EBV_B cells from HDs and RRMS patients were prepared with the Universal Plus mRNA-Seq kit (Tecan) and sequenced on a NovaSeq X with paired-end 150 bp reads (2 $\times$ 150 bp). Raw sequencing reads were processed using fastp to remove adapter sequences, trim low-quality bases, and discard reads with a mean Phred quality score < 20.[85] High-quality reads were subsequently pseudoaligned with an index consisting of the human reference genome (GRCh38.p14; GENCODE release 48) and the EBV B95-8 genome (NCBI RefSeq GCF_002402265.1) and quantified at the gene level using Kallisto.[86] Differential expression analysis was performed with edgeR,[87] applying a quasi-likelihood negative binomial generalized log-linear model (glmQLfit). Genes with FDR < 0.05 were considered differentially expressed. Principal component analysis (PCA), Volcano plot, and Heat map of the mRNA expression were generated using Wei Sheng Xin (Newcore Biotech) and CytoNavigator (NovelBio).

Western blotting

Cells were lysed with RIPA buffer (EpiZyme, Shanghai, China) including protease inhibitors cocktail (EpiZyme), and protein concentrations in the extracts were measured with a BCA protein Assay kit (Pierce, Thermo Scientific). Protein samples were electrophoresed on 10% SDS-polyacrylamide gels and then transferred to polyvinylidene fluoride membranes (Merck, Rahway, USA). The membranes were then incubated at 4 °C overnight with anti-MBP antibody (BioLegend), anti-PSMB8 antibody (Proteintech, Wuhan, China), anti-LC3A/B antibody (CST, Massachusetts, USA), anti-α-tubulin antibody (Proteintech) or anti-beta actin antibody (Proteintech) after being pre-blocking incubated with 5% non-fat milk. After several washes, the blots were then probed with an appropriate secondary antibody for 1 h at room temperature. Protein bands were revealed by chemiluminescence and recorded on an Amersham™ ImageQuant™ 800 imaging system (Cytiva, USA).

Proteomic analysis

The EBV_B cells were lysed in 50 μl of a solution containing 2% sodium dodecyl sulfate (SDS), 2% sodium deoxycholate (SDC), 2% dodecyl β-D-maltoside (DDM), 50 mM triethylammonium bicarbonate (TEAB), pH 8.2, 50 mM dithiothreitol (DTT) for 10 min at a temperature of 95°C and 700 rpm followed by treatment with high intensity focused ultrasound (Hielscher Ultrasonics GmbH) for 1 min (100% amplitude, 60% cycle time). Subsequently, the supernatant was reduced and alkylated for 30 min at 30°C and 700 rpm by the addition of tris(2-carboxyethyl)phosphine and 2-chloroacetamide to a final concentration of 5 mM and 15 mM, respectively. Afterwards, the samples were diluted with pure ethanol to achieve a final concentration of 60% ethanol by volume, and the following processing steps were performed on a KingFisher Flex System (Thermo Fisher Scientific). Carboxylated magnetic beads (Cytiva) are washed three times with water to remove any impurities. Subsequently, the samples were incubated with a 10-fold excess of magnetic beads (w/w) for 30 min at room temperature. After the incubation, the beads were washed three times for three minutes with 80% ethanol. The enzymatic digestion was initiated by adding trypsin in 50 mM TEAB (pH 8.5) to the beads, which were then incubated at 37°C overnight at 700 rpm. The peptide-containing solution was collected, and the magnetic beads were washed once with pure water. The two elutions were combined and dried down. The dried samples were resolubilized in 20 μl of MS-solvent (3% acetonitrile, 0.1% formic acid) and 1 μl of indexed retention time peptides (iRT; Biognosys AG) was spiked in each sample for future retention time calibration.

Mass spectrometry analysis was performed on an Orbitrap Exploris mass spectrometer (Thermo Scientific) equipped with a Digital PicoView source (New Objective) and coupled to a M-Class UPLC (Waters). Solvent composition at the two channels was 0.1% formic acid in water for channel A and 0.1% formic acid in acetonitrile for channel B. For each sample 1 μL of peptides were loaded on a trap column (MZ Symmetry C18, 100 Å, 5 μm, 180 μm x 20 mm, Waters AG) that was connected to an analytical column (MZ C18 HSS T3, 100 Å, 1.8 μm, 75 μm x 250 mm, Waters AG). The peptides were eluted at a flow rate of 300 nl/min by

a gradient from 5% to 22% B in 80 min, 32% B in 10 min and 95% B in 1 min. Samples were acquired in a randomized order. The mass spectrometer was operated in data-independent mode (DIA), acquiring a full-scan MS (396–1000 m/z) at a resolution of 60'000 at 200 m/z. Followed by HCD (higher-energy collision dissociation) fragmentation on 70 windows with 8 m/z width between 400 and 960 m/z. The MS2 resolution was set to 30'000 and a normalized collision energy of 30% was used. The samples were acquired using internal lock mass calibration on m/z 371.1012 and 445.1200. The mass spectrometry proteomics data were handled using the local laboratory information management system (LIMS).[88]

The identification and quantification of proteins from MS data was performed using the DIA-NN workflow (version 1.8.2).[89] The following parameters for the library-free search were used: precursor charge +2 and +3, precursor mass range 350 m/z to 1500 m/z, fragment mass range 200 m/z to 1800 m/z, mass accuracy MS1 15 ppm, MS2 20 ppm, enzyme specificity trypsin/P allowing one missed cleavage, fixed modification carbamidomethylation of cysteine. The in-silico spectra were generated using a canonical protein database for human and Epstein-Barr virus, concatenated with common protein contaminants (p38645_db1_HumanNEBVG_1spg_ 20250523.fasta, taxonomy ID9606 and ID10376, release date 20250523) and the maximum false discovery rate (FDR) was set to 0.1.

The R package prolfqua[90] was used to analyze the differential expression and to determine group differences, confidence intervals, and false discovery rates for all quantifiable proteins. Starting with the report.tsv file generated by DIA-NN, which does report the precursor ion abundances for each raw file, we determined protein abundances by first aggregating the precursor abundances to peptidoform abundances. Then, we employed the Tukeys-Median Polish to estimate protein abundances. Furthermore, before fitting the linear models, we transformed the protein abundances using the variance stabilizing normalization.[91]

Tissue-specific gene enrichment analysis

Enrichment of human tissue-specific genes among the source proteins of the peptides was done using R with the R package "TissueEnrich".[80] Human tissue-specific genes used for the analysis were defined by processing the RNA-seq data across 29 human tissues from the GTEx dataset[92] using an algorithm from the Human Protein Atlas.[81] A hypergeometric test was used to determine whether the tissue-specific genes are enriched among the input genes corresponding to the source protein list of the peptides. The result of the enrichment analysis was visualized using R with the R package "Heatmaply".[82]

Proliferation assay

Peptides used in this study for stimulation purposes were synthesized with N-terminal acetylation and C-terminal amide (Peptides & Elephants, Henningsdorf, Germany; GL Biochem, Shanghai, China): $MBP_{(78-90)}$: GRTQDENPVVHFF, $MBP_{(83-90)}$: ENPVVHFF, $MBP_{(83-99)}$: ENPVVHFFKNIVTPRT, $MBP_{(91-106)}$: KNIVTPRTPPPSQGKG, $MBP_{(91-114)}$: KNIVTPRTPPPSQGKGR GLSLSRF, $MOG_{(35-55)}$: MEVGWYRSPFSRVVHLYRNGK, other MS brain MBP peptides, and CEF II peptide pool. Peptide stimulation assays of PBMCs and TCCs were conducted as previously described.[10] $CD45RA^-$ PBMCs were isolated by negative selection using CD45RA microbeads, human (Miltenyi) and were then seeded at 2×10^5 cells/well in 200 μl X-VIVO 15™ medium (Lonza) in 96-well U-bottom plates (Greiner Bio-One), and MBP peptides were added at a final concentration of 10 μM. 5-10 replicate wells were tested per condition, and anti-CD2/CD3/CD28 antibody-loaded MACSibead particles (Miltenyi) were used as a positive control. A pan-HLA-DR-specific antibody (L243) was added in some conditions to block the function of HLA-DR molecules at a final concentration of 10 μg/ml. Proliferation was measured at day 7 by ^{3}H-thymidine (Hartmann Analytic, Braunschweig, Germany) or BrdU (Roche) incorporation assay. The proliferation strength is depicted as a stimulatory index (SI). For the TCCs, TCCs (2×10^4 cells/well) were seeded with irradiated (300 Gray) BLS-DR2a or -DR2b cells (5×10^4 cells/well) as APCs in 200 μl X-VIVO 15™ medium (Lonza) in 96-well U-bottom plates (Greiner Bio-One) and stimulated with individual or pooled MBP peptides at a final concentration of 10 μM. Target antigens MBP_{83-99} and anti-CD2/CD3/CD28 antibody-loaded MACSibead particles (Miltenyi) were used as positive control of stimulation. Proliferation of TCCs was measured at day 3 by ^{3}H-thymidine (Hartmann Analytic) incorporation assay.

Cytokine measurements

Supernatants were harvested from $CD45RA^-$ PBMCs on day 7 or from TCCs on day 3 after peptide stimulation. Cytokines in the supernatants were measured with a bead-based immunoassay using a LEGENDplex Multi-analyte Flow Assay kit (#741028, Biolegend) according to the manufacturer's instructions. ELISpot assays (Human IFN-γ (ALP), Mabtech) were set up by washing the plates four times with PBS as indicated in the manufacturer's protocol. TCCs (2×10^4 cells/well) were seeded with irradiated BLS-DR2b cells (5×10^4 cells/well) as APCs in 200 μl X-VIVO 15™ medium (Lonza) in 96-well U-bottom plates (Greiner Bio-One) and stimulated with MBP peptides. Anti-CD2/CD3/CD28 antibody-loaded MACSibead particles (Miltenyi) were used as a positive control of stimulation. Cells were incubated for 44h at 37°C in 5% CO_2 incubator before developing the assay according to the manufacturer's protocol. Plates were left to dry for 48h and subsequently read using the Mabtech IRIS ™ FluoroSpot/ELISpot reader.

Flow cytometric analysis

For analyzing DR2a, DR2b, and HLA-DR expression levels on primary B cells and EBV-transformed B cell lines, PBMCs from $HLA\text{-}DR15^+$ donors and EBV-transformed B cell lines were incubated with human IgG (Sigma-Aldrich) to block unspecific

antibody binding to Fc-receptors, labeled with Live/Dead® Aqua (Invitrogen), and then stained for surface marker using fluorochrome-conjugated antibodies, including Alexa Fluor 488-conjugated anti-DR2a antibody (5 μg/ml, One Lambda, Thermo Fisher Scientific), Alexa Fluor 647-conjugated anti-DR2b antibody (5 μg/ml, One Lambda, Thermo Fisher Scientific), anti-human CD3 antibody (OKT3, Biolegend), anti-human CD19 antibody (HIB19, Biolegend) and anti-human HLA-DR antibody (L243, Biolegend), at 4°C. Cells were washed twice after staining and resuspended with cold PBS containing 2 mM ethylenediamine tetraacetic acid (EDTA, AppliChem) and 2% FCS (Eurobio). Measurements were performed using LSR Fortessa Flow Cytometer (BD Biosciences) and data analyzed with FlowJo (Tree Star). Additional fluorochrome-conjugated antibodies, including anti-human CD4 antibody (OKT-4, Biolegend), anti-human CD8 antibody (SK1, Biolegend), and anti-human CD14 antibody (HCD14, Biolegend), were used for analyzing different cell subsets.

T cell cloning and identification

To generate $CD4^+$ TCCs that recognize MBP peptides, PBMCs from 4 $HLA\text{-}DR15^+$ relapsing-remitting multiple sclerosis (RRMS) patients were stained with CFSE, and $CD45RA^-$ PBMCs were then isolated using CD45RA microbeads, human (Miltenyi) and stimulated with MBP peptide pool at a concentration of 10μM for each peptide. Proliferating ($CFSE^{dim}$) $CD4^+$ T cells were sorted on day 11 as single cells in 96-well U-bottom plates using SH800S Cell Sorter (Sony) and expanded as previously described.[10] The reactivity of the expanded TCCs to MBP peptides, the phenotype of the TCRVβ chain of the TCCs, the functional phenotype of the TCCs, and the restriction of the TCCs to the DR2a or DR2b were tested as previously described.[10]

STATISTICAL ANALYSIS

Statistical analyses were performed using GraphPad Prism 8.0 (GraphPad). Unpaired t-test was used for statistical analyses. Data were expressed as mean and mean ± SEM, which are indicated in the figure legends. The data were considered statistically significant when differences achieved values of $p < 0.05$. The p values are reported in the figures where significant.

Supplemental figures

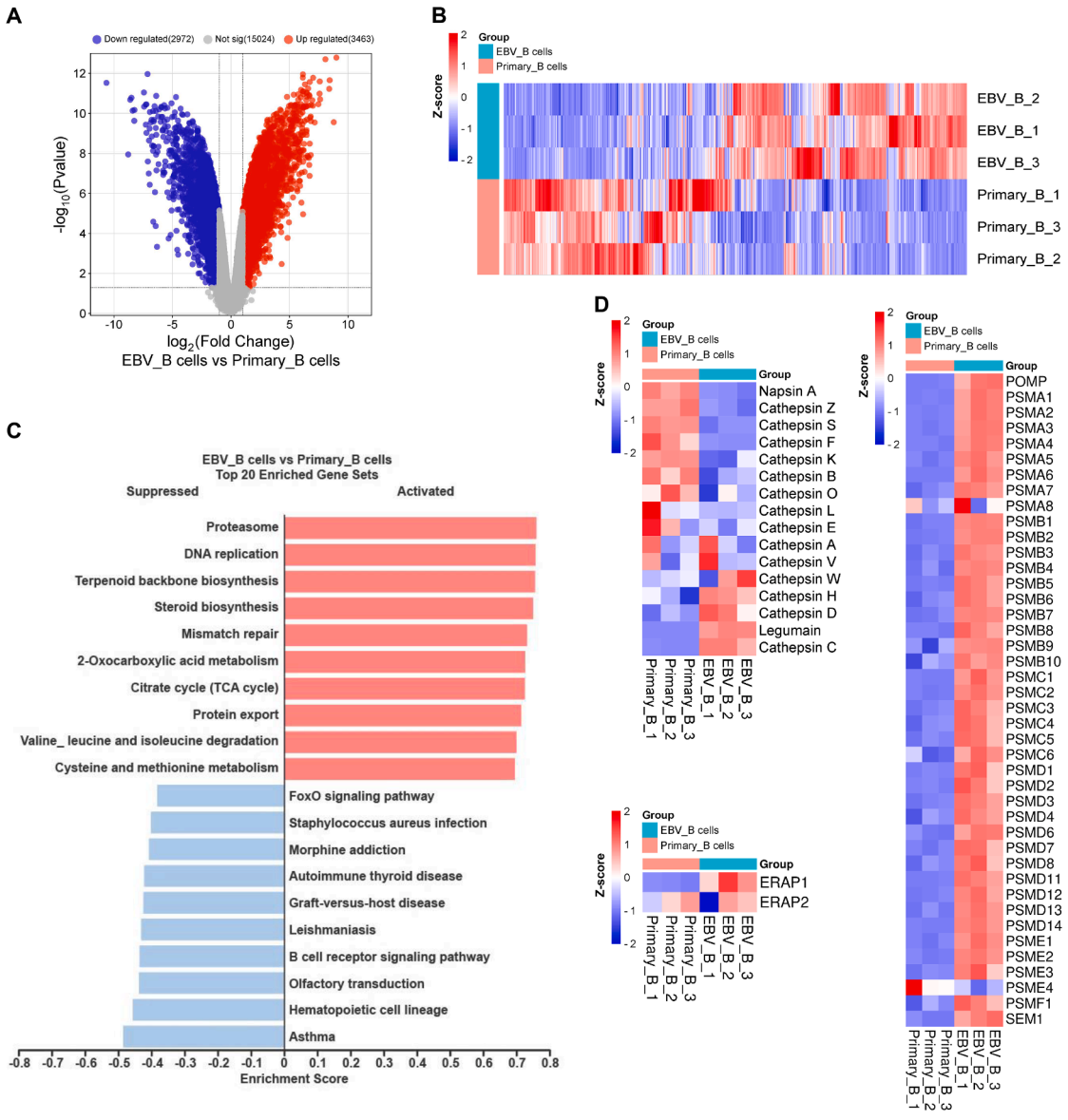

Figure S1. EBV infection alters the transcriptome in B cells, related to Figure 1

(A) Volcano plot of RNA-seq results showing significantly differentially expressed genes between primary B cells and EBV-transformed B cells (log_2 ratio ≥ 0.5 with $p \leq 0.01$). Significant indicates genes with $|log_2$ ratio$| \geq 0.5$ and $p \leq 0.01$.

(B) Heatmap showing the different expression levels of the genes in primary_B cells and EBV_B cells.

(C) Gene set enrichment analysis reveals the top 20 enriched gene sets in B cells after EBV infection. Upregulated genes are indicated by red and the down-regulated by blue.

(D) Heatmap showing the changed expression of cathepsins, endosomal proteases, and ERAP1/2 in EBV_B cells.

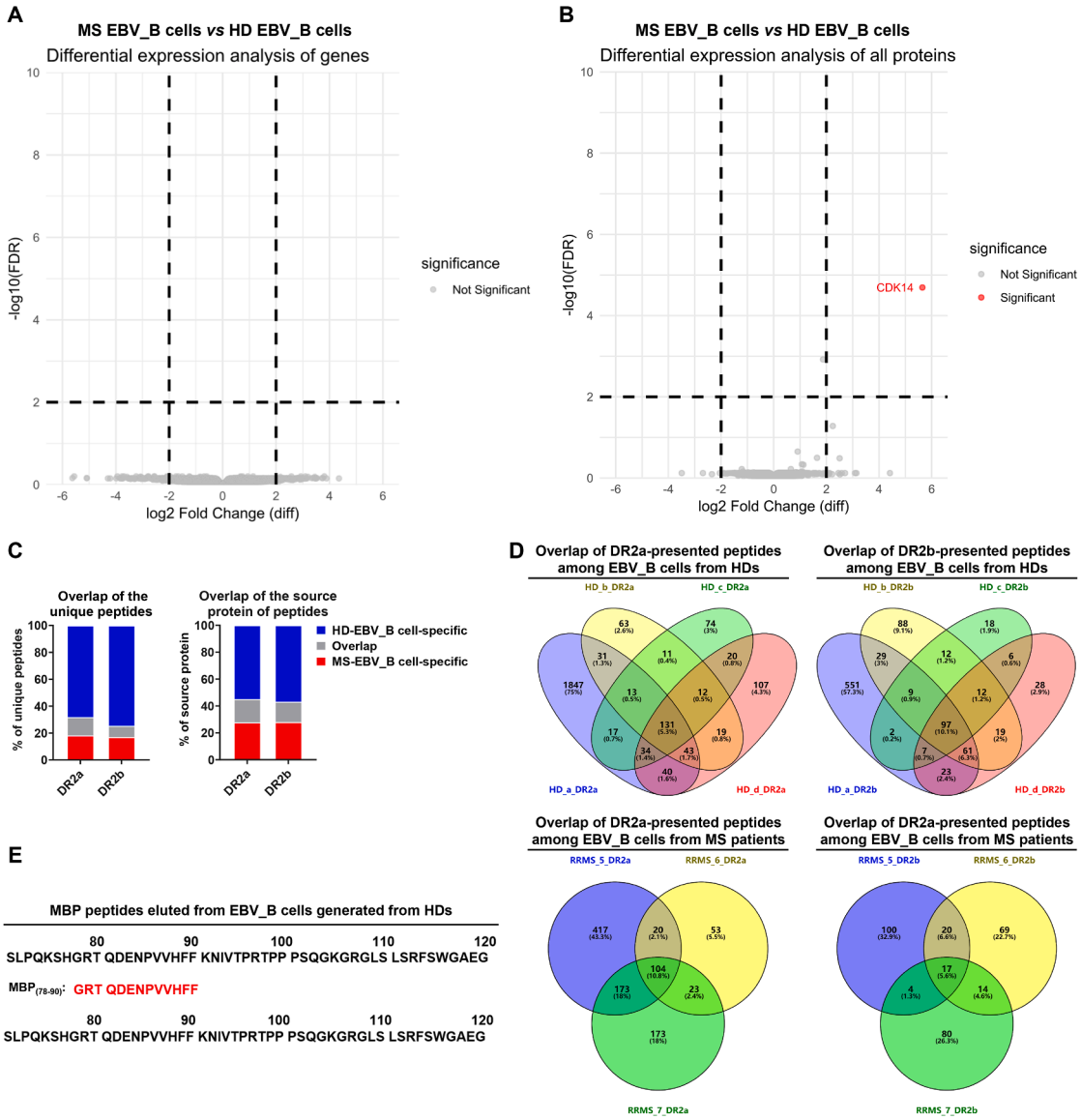

Figure S2. Fewer MBP peptides are eluted from HLA-DR15 molecule in EBV_B cells from HDs, related to Figure 1 and Tables S2 and S3

(A) Volcano plot of RNA-seq results showing significantly differentially expressed genes between EBV_B cells from HLA-DR15$^+$ HDs and MS patients.

(B) Volcano plot of proteomic results showing significantly differentially expressed proteins between EBV_B cells from HLA-DR15$^+$ HDs and MS patients.

(C) Overlap of DR2a- and DR2b-presented unique peptides and their source proteins between EBV_B cells from HLA-DR15$^+$ HDs and MS patients.

(D) Overlap of DR2a- or DR2b-presented unique peptides among EBV_B cells from different HLA-DR15$^+$ HDs or MS patients.

(E) One MBP peptide was eluted from the HLA-DR15 molecule in EBV_B cells from HDs.

Data are expressed as mean.

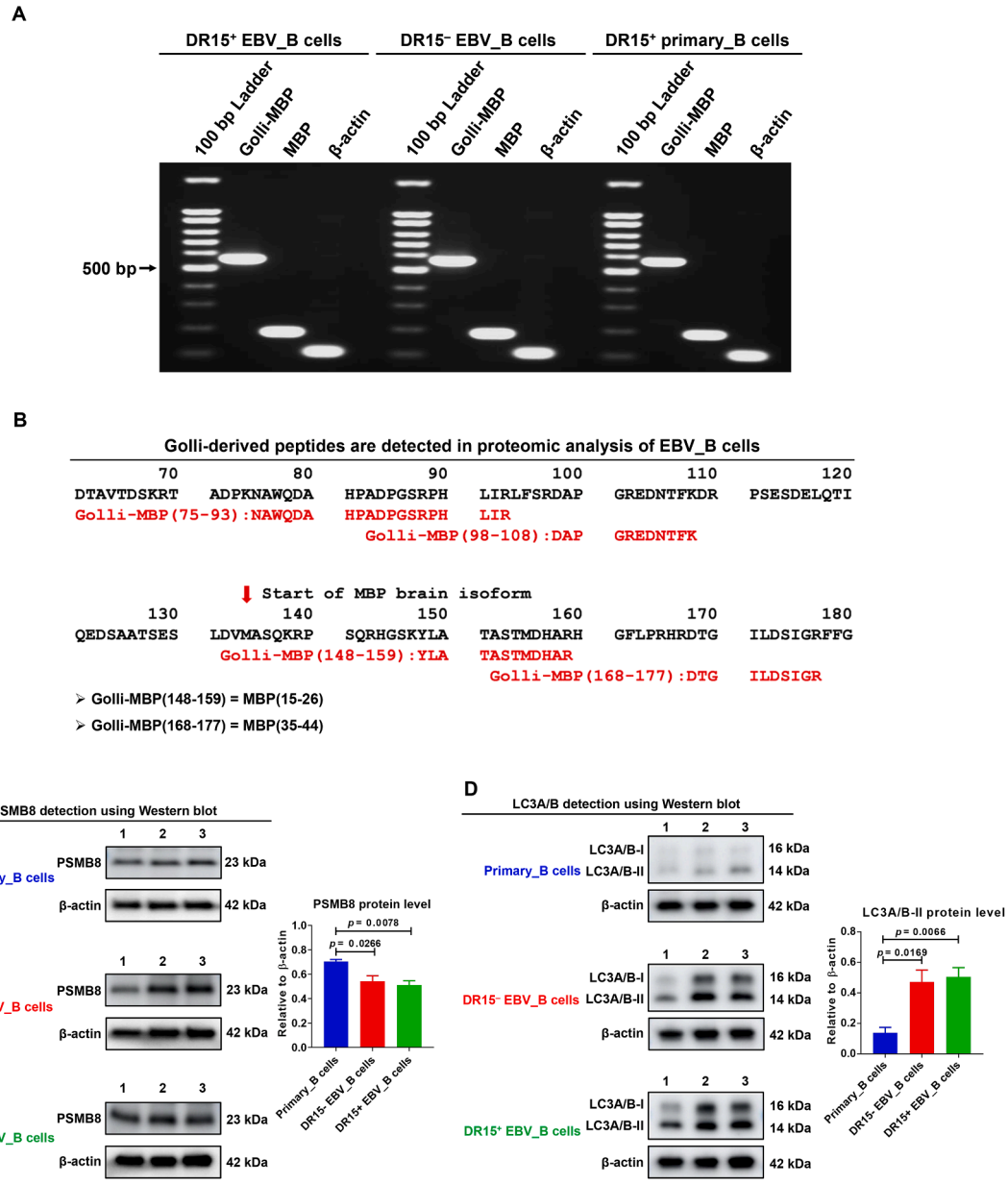

Figure S3. Golli-MBP is expressed in primary_B cells and is degraded through the synergistic action of PSMB8 and autophagy after EBV infection, related to Figure 1

(A) Analysis of Golli-MBP expression in primary_B cells and EBV_B cells using PCR.

(B) Golli-derived peptides are detected in proteomic analysis of EBV_B cells.

(C) Expression of PSMB8 protein in primary_B cells, DR15^{-} EBV_B cells, and DR15^{+} EBV_B cells.

(D) Expression of LC3A/B protein in primary_B cells, DR15^{-} EBV_B cells, and DR15^{+} EBV_B cells.

Data are expressed as mean ± SEM, and *p* values were determined by unpaired *t* test.

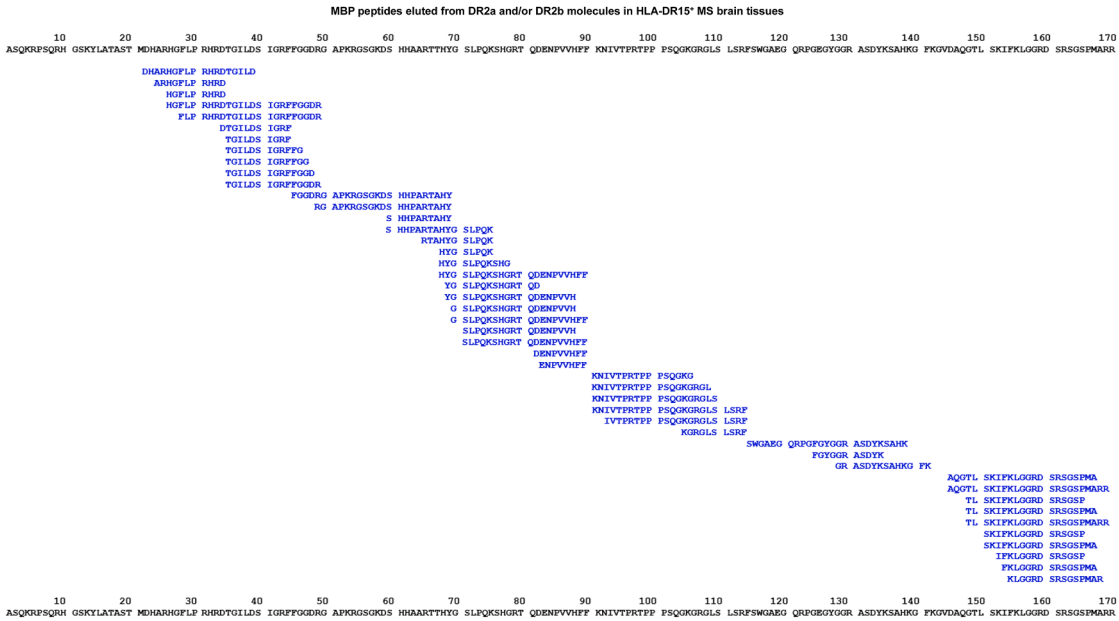

Figure S4. DR2a/DR2b-presented MBP peptides in MS brain tissues cover nearly the entire sequence of the most abundant isoform of MBP, related to Figure 2 and Table S4

Unique MBP peptides eluted from DR2a and DR2b in HLA-DR15^{+} MS brain tissues.

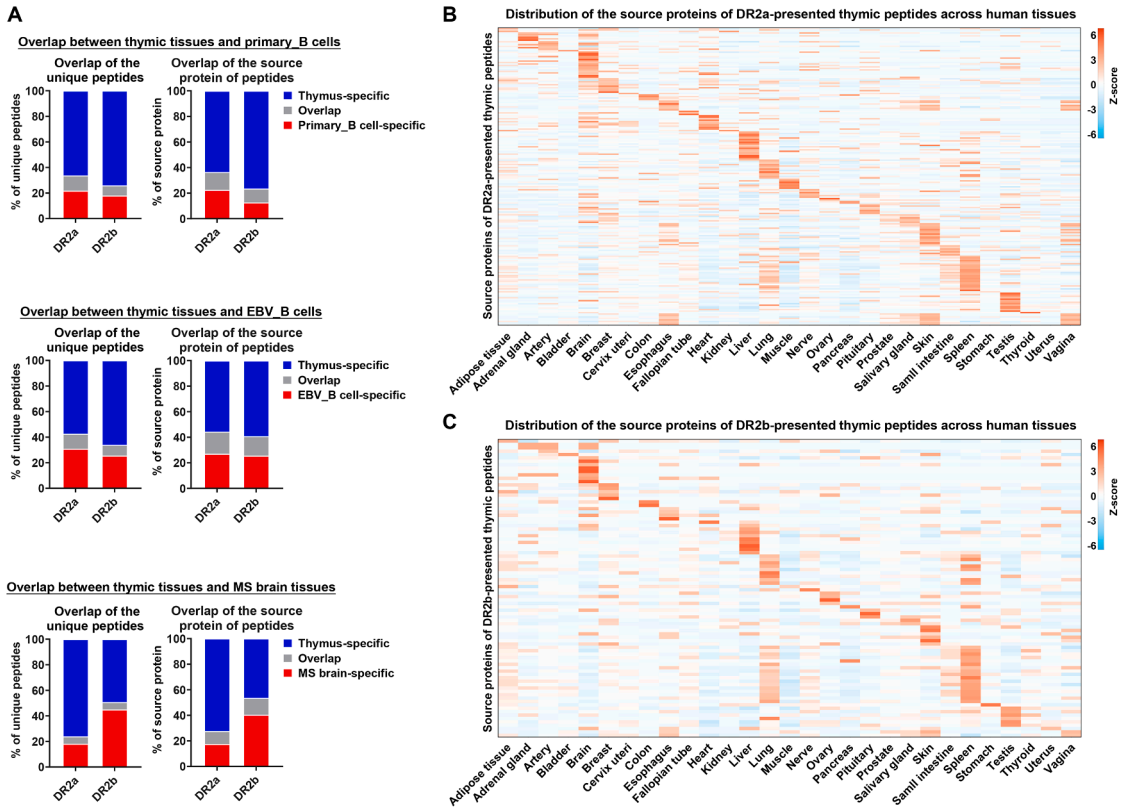

Figure S5. The source proteins of eluted thymic peptides are distributed in all human tissues, related to Figure 4 and Table S6

(A) Overlap of DR2a- and DR2b-presented unique peptides and their source proteins between thymic tissues and primary_B cells/EBV_B cells/MS brain tissues.

(B) Distribution of the source proteins of DR2a-presented thymic peptides across human tissues.

(C) Distribution of the source proteins of DR2b-presented thymic peptides across human tissues. Data are expressed as mean.

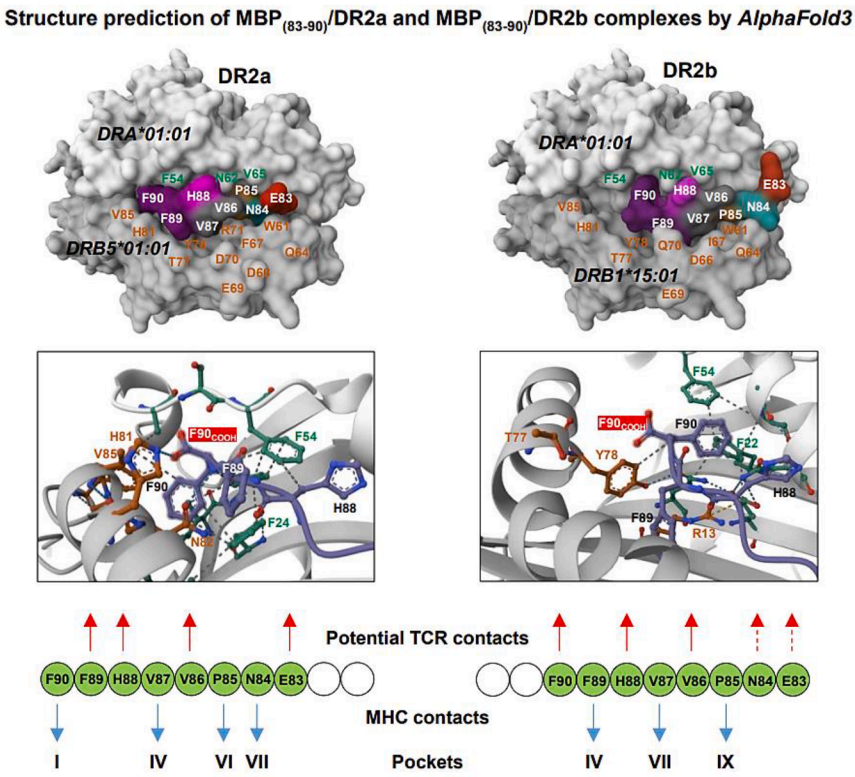

Figure S6. 1642KA_TCC1B3 shows a specificity to the N-terminal part of the peptides MBP$_{(83–90)}$ presented by DR2 and DR2b, related to Figure 6

Prediction of the structure of MBP$_{(83–90)}$/DR2a and MBP$_{(83–90)}$/DR2b complexes by AlphaFold3 and the potential contact positions for 1642KA_TCC1B3 TCR and DR2a/DR2b in the peptide MBP$_{(83–90)}$, respectively.